Imperial College London

Measuring the mass of the topological defect in $(\lambda\phi^4)_{1+2}$ model using the 3D Ising Model and Monte Carlo Simulations

Eliana Lambrou

Supervisor:

Dr. Arttu Rajantie

Submitted in partial fulfilment of the requirements for the degree

of Master of Science of Imperial College London

September 20, 2011

Abstract

The mass of this topological defect created in the $(\lambda\phi^4)_{1+2}$ model was measured using the 3-dimensional Ising model due to the fact that the specific spin model and the $\lambda\phi^4$ model live in the same universality class. In fact, the implementation of the model was done using Monte Carlo Simulations and the mass was measured using two different non-perturbative methods. The first one involved the free energy of the defect found by the difference between the free energies of the system with twisted and periodic boundary conditions and it had already been used in other works for finding similar quantities. The second method was a new one that was checked to be working in $(1+1)$ dimensions and involves correlation functions from which the mass can be extracted directly. The results between the two methods have a significant difference which might be explained by the finite lattice effect.

Acknowledgements

This dissertation would not have been possible without the valuable supervision, support and useful comments on my work from my supervisor, Dr. Arttu Rajantie. I am also heartily grateful to Dr. David Weir, for the long hour conversations on the topic and his overall help. Furthermore, I owe my deepest gratitude to my parents who supported me both morally and financially throughout this year and to everyone who supported me in any respect during the completion of this dissertation. Lastly, I would like to thank my friend Niki, who has always been supportive, encouraging me to do my best recalling the famous words that "Striving for success without hard work is like trying to harvest where you haven't planted"

Contents

Chapter 1

Introduction

The whole world is governed by physical laws. Due to the curious nature of the human beings, people never stopped asking what the underlying physics behind what we see and even importantly behind what we are not able to see is. From the microscopic to the macroscopic scales, theoretical physicists develop models hoping that a better understanding of our Universe will be achieved. The hope that a Grand Unified Theory, i.e. a theory that will unify the strong with the electroweak force at all energy scales, can be achieved let many physicists search for a new gauge symmetry that will give a unified coupling constant. One candidate that might achieve this dream is String Theory: a quite recent area of physics but yet one of the most revolutionary proposals that has ever occurred. Any model of the GUT predicts the existence of topological defects such as cosmic strings, monopoles and domain walls. The latter, has been investigated by cosmologists who developed many cosmological models to explain the structure of our universe and it believed that as the hot universe was cooled down a domain wall was formed which has an effect in the homogeneity of the present universe. Furthermore, the domain wall gets a "string nature" in the problem of the confinement of QCD at the point where the phase transition occurs between the deconfinement and confinement regime.

In the first half of the 19th century the evolutionary idea that the world we live in is

not classical but quantum mechanical raised new perspectives of all the theories that were postulated by then. Quantum field theory was proven to be one of the most important fields that contributed the most in the understanding of the behaviour of our universe. However, the quantization of a field theory is not always trivial and many times arises complex problems. The main way to estimate quantized solutions is by applying perturbation theory around the classical solution. Even though this has been proven powerful, for non-linear systems perturbation theory ignores many effects which are actually important. Thus finding a non-perturbative way to examine quantization of a system is of high importance.

Non-linear systems take many forms. Theoretical physicists, during their attempt to find a Grand Unified Theory, came up with revolutionary ideas that changed the whole view of the universe. By studying the topology of the non-linear field equations, which arise from different field theories, they introduced the idea of topological solitons. Following, they became able to characterize interfaces, kinks, vortices or monopoles that were present in the theories of their research as topological defects. Nowadays, a significant number of people is working on them and many papers regarding them have been published.

In this dissertation, our focus is on interfaces created in three dimensions which can be visualized as an extended kink in 2 dimensions, i.e. a domain wall or a spatial t' Hooft loop. When someone deals with the 3-dimensional Ising Model, which is a spin statistical model, it can easily be seen that by investigating the magnetization which is an order parameter, a second order phase transition occurs in the phase where the global $\mathbb{Z}_2$ symmetry is spontaneously broken. By changing the boundary conditions of the model, an interface is created in the broken phase which is considered to be the topological defect in the theory and its properties can be investigated. The main task is to find its mass using two different methods, out of which only the one has already been tested in previous

works. Both methods are non-perturbative methods so no effects are excluded. The first method is that of the finite free energy differences which was applied many times to a variety of field theories but has the disadvantage that all the measurements have to be taken from a point where the free energy is known and so it has a cost in the computational time. The new method that is tested here was first proposed in [1] in which it was shown to be working in $(\lambda\phi^4)_{1+1}$ model. In this work, the latter method is extended to $(\lambda\phi^4)_{1+2}$ model which is implemented by the 3-dimensional Ising Model. The behaviour of the two models is the same close to the critical point, since they live in the same universality class.

Interfaces created in theories with phase transitions have gained the interest of many people and they seem to have a wide range of applications in various fields. They were investigated in biology, chemistry and soft condensed matter especially in phase transitions between two different fluids or fluids and their vapours [2], [3], [4]. However, our motivation to investigate further the interfaces created as topological defects, comes mostly from the perspective of theoretical physics and specifically cosmology and the problem of the confinement in QCD. Interfaces that are created in the $\lambda\phi^4$ theory have gained the interest of cosmologists since it is believed that a domain wall was created as a topological defect in the symmetry-breaking phase transition of the radiation-dominated FRW Universe at early times and thus it becomes a candidate for the structure formation of the Universe [5]. On the other hand, the interface that is created in the 3D Ising Model by imposing antiperiodic boundary conditions, has been investigated by people that base their research in the problem of the confinement in QCD. In QCD, it is well-known that a phase transition occurs between the confining and the deconfining regime. Thus, the investigation of this transition, it is believed that can lead to the understanding of the confinement problem. In fact, this phase transition takes place in the broken phase of the centre symmetry of the Yang-Mills theory which is a gauge theory. Using Group Theory as a powerful tool, it can be shown that actually the $d+1$-dimensional Yang-Mills gauge theory lives in the same universality class as the d-dimensional Ising Model close to the

critical point. Thus the interface created can be considered as a spatial t' Hooft loop which scales with the surface area. So, a string realization of the confining-deconfining transition is achieved.

The structure of the dissertation is given as below: Firstly, the main ideas behind both the 3D Ising Model and the Quantum Field Theory model which is considered here are explained in Chapter [2]. A small introduction to the topological defects can be read in Chapter[3] where also a brief discussion between the use of the model in the understanding of the confinement problem in QCD and cosmology is given. Following, the two methods for measuring the mass of the domain wall are presented in Chapter[4]. Then the algorithm that was used for the implementation and results of the 3D Ising Model with periodic boundary conditions are shown in Chapters [5] and [6] respectively. Finally, in the last two chapters, results of the mass of the domain wall obtained using the two different methods are shown and discussed and the final conclusion with possibilities of further work that can be done are presented.

Chapter 2

The $(\lambda\phi^4)_{1+2}$ model and its correspondence to the 3D Ising Model

2.1 The Ising Model

Statistical mechanics play an important role in physics, therefore toy spin models based on them were used throughout the years for the investigation of a wide range of physical aspects in a variety of fields of physics. The most well-known model for finding phase transitions and basic physical properties such as the average magnetization or the energy of a system is the Ising Model. The basic idea behind this model is to consider the system as a lattice in D-dimensions with N^D lattice points at each of which there is a spin that points either up or down, i.e it can take values of the group $\mathbb{Z}_2$. The Ising Model has been investigated for many years since it is one of the most successful but yet simple models to develop, especially after the development of supercomputers or even simple computers which can do calculations extremely quickly. The 1D and 2D Ising Models had been investigated in depth both analytically and numerically and there was a very accurate match between the values of the properties measured using both methods. For

further reading on it and especially an extent of the case of $D = 2$ Ising Model one can refer to [6]. In $D \geq 3$ the Ising Model becomes too complicated and it does not have an analytical solution, however for the case of 3-dimensions, very accurate numerical results have been published over the years and even phenomenological approaches were done such as the one in [7].

Even though, the Ising Model was first introduced as a ferromagnetic model, it was then extended to many areas of physics, in which many physical models were described and investigated using the statistical nature of it. Some examples are those of the condensed matter and especially the investigation of spin glasses and theoretical physics in which the investigation of gauge theories is taking place using the duality between the Ising Model and the gauge Ising Model.

The contribution of the Ising Model to Quantum Field Theory is significant enough, leading to an enormous amount of papers being published in which the specific spin model in D dimensions, mostly in D=2 to 4, is investigated and it is related to different Quantum Field Theory models. For the purposes of this dissertation, the 3D Ising Model will be used for reasons that will be stated followed by some basic concepts in Statistical Mechanics and some properties of the model.

2.1.1 Basic Statistical Mechanics

For better understanding of the Ising Model it is useful to state a few basic statistical concepts that are important.

Firstly, let us recall that the Boltzmann weight is given by $e^{-\mathcal{H}/kT}$ where $\mathcal{H}$ is the Hamiltonian (energy) of the system, k is the Boltzmann constant and T is the temperature. By defining $\beta = 1/kT$ this reduces to $e^{-\beta\mathcal{H}}$. The partition function, which plays a very

important role in statistical physics and probabilities, is then defined as the sum over all the Boltzmann weights as in Equation (2.1):

$$Z = \sum_{s} e^{-\beta \mathcal{H}(s)}. \tag{2.1}$$

The partition function is of a great importance since it renormalizes the probability distribution given by:

$$\mathcal{P}(s) = \frac{1}{Z} e^{-\beta \mathcal{H}(s)} \tag{2.2}$$

and one can find expectation values of observables using it by the standard form of thermal averages of observables:

$$\langle \mathcal{O} \rangle = \frac{1}{Z} \sum_{s} \mathcal{O} e^{-\beta \mathcal{H}}. \tag{2.3}$$

In statistical physics the free energy, F, plays an important role and all observables can be expressed as derivatives of it. It is defined to be proportional to the natural logarithm of the partition function as shown in Equation (2.4):

$$F = -kT \ln Z. \tag{2.4}$$

2.1.2 Basic Properties of the Ising Model

In the Ising model it is assumed that the magnetic moments are highly anisotropic, such that the spin at each lattice point can take one of the two available spin values (e.g.± 1), i.e. the spins can point either up or down. Each spin interacts with the nearest neighbouring spins and the Hamiltonian is given by:

$$\mathcal{H} = -J \sum_{<i,j>} S_i S_j - \mu B \sum_{i} S_i \tag{2.5}$$

where J is the interaction strength, S_i are the spins, μ is the magnetic moment, B is the applied external magnetic field and by $< i, j >$ the sum over neighbouring spins is implied.

By setting $B = 0$ so that there is no external field, thermodynamic quantities can be measured such as the average magnetization of the system given by Equation (2.6):

$$M = \frac{1}{N} \sum_{i=1}^{N} S_i \tag{2.6}$$

or the internal energy U which is given by the average of the Hamiltonian. In the case of the 3D Ising Model the Hamiltonian explicitly is given by the following equation:

$$\mathcal{H} = -J \sum_{i=1}^{3} S_i S_{i+1}. \tag{2.7}$$

2.2 The $\lambda\phi^4$ model

2.2.1 The action of the model in the continuum

In the world of high energy physics one of the most well known models is that of the massive self-interacting scalar field theory, i.e. the $\lambda\phi^4$ model. The Lagrangian of the theory might appear to be slightly different in papers that were published over the years, however it describes the same model and the main physical concepts behind it remain unchanged. In this dissertation the following Lagrangian in (1+2) dimensions is considered:

$$\mathcal{L} = \frac{1}{2}(\partial_\mu \phi)(\partial^\mu \phi) + \frac{1}{2} m^2 \phi^2 - \frac{\lambda}{4!}\phi^4 \tag{2.8}$$

where the potential, V, is identified to be $V(\phi) = -\frac{1}{2}m^2\phi^2 + \frac{\lambda}{4!}\phi^4$; $\lambda > 0$

Then the action in Minskowski space is given by :

$$\int dtd^2x\mathcal{L} \tag{2.9}$$

One can easily go to Euclidean space by Wick rotating the action, that is by imposing $t \to -i\tau$.

Then the action becomes:

$$\begin{aligned} iS &= \int dtd^2x \left[\frac{1}{2}\left(\frac{\partial\phi}{\partial t}\right)^2 - \frac{1}{2}\left(\frac{\partial\phi}{\partial x_i}\right)^2 - V(\phi)\right] \\ &= -\int d\tau d^2x \left[\frac{1}{2}\left(\frac{\partial\phi}{\partial \tau}\right)^2 + \frac{1}{2}\left(\frac{\partial\phi}{\partial x_i}\right)^2 + V(\phi)\right] \\ &= -\int d^3x \left[\frac{1}{2}\left(\frac{\partial\phi}{\partial x_i}\right)^2 + V(\phi)\right] \\ &= -S_E \end{aligned} \tag{2.10}$$

where S_E is the Euclidean action since in the 3D Euclidean space the metric is just $g_{ij} = diag(1,1,1)$ and thus time and space are indistinguishable.

2.2.2 The $\lambda\phi^4$ model on a lattice

So far the field theory is considered in the continuum. However, in order to implement it using a spin model, it has to be discretized on a lattice. All that is needed to be done is to divide the lattice extension into small intervals of length α, transform all the integrals into sums over the whole lattice space and replace continuous derivatives by their mathematical definition. That is, mathematically the following are done:

1. x = L_1/α ; y = L_2/α ; z = L_3/α

2. $\int$ dx $\to \alpha \sum_{n=0}^{L/a}$ and for a cubic lattice : $\int$ $d^3x \to \alpha^3 \sum_{n=0}^{L^3/a}$

3. $\frac{\partial\phi}{\partial x} = \frac{\phi[(n+t)\cdot\alpha]-\phi[n\cdot\alpha]}{\alpha}$

For our convenience α is set to 1, thus the discretized Euclidean action becomes :

$$S_E = -\sum_{n,t}\phi(n)\phi(n+t) + \sum_{n}\left[\left(3-\frac{m^2}{2}\right)\phi(n)^2 + \frac{\lambda}{4!}\phi(n)^4\right] \tag{2.11}$$

In field theory, the path integral formulation proposed by Dirac and completed by Feynman, became very important since it provides symmetry in space and time. One can start from simple quantum mechanics and derive the path integral which can be thought of as a sum over all possible configurations of a system that satisfy certain boundary conditions. Its importance in Quantum Field Theory is mostly realized when someone wants to measure values of observables which are found using :

$$\langle\phi(x)\rangle = \frac{1}{Z}\int \mathcal{D}\phi e^{-S_E}\phi(x). \tag{2.12}$$

where $\int \mathcal{D}\phi$ is considered to be the integral over all possible field configurations in all directions including space and time and $Z[J]$ is the generating functional given by:

$$Z[J] = \int \mathcal{D}\phi e^{iS+i\int d^dx J(x)\phi(x)}. \tag{2.13}$$

In the absence of J, this can be considered as

$$Z[J] = \int \mathcal{D}\phi e^{iS} = \int \mathcal{D}\phi e^{-S_E} \tag{2.14}$$

In the discretized case this becomes

$$Z[J] = \sum_{x,y,z} e^{-S_E} \tag{2.15}$$

Comparing Equations (2.1) and (2.15) one can see that the generating functional in Quantum Field Theory is the equivalent of the partition function in Statistical Mechanics by identifying $S_E = \beta\mathcal{H}$

2.3 Using the Ising Model in $\lambda\phi^4$ theory

It is natural for someone to address the question why we can use the Ising Model to implement the ϕ^4 theory. The answer to this is simply that the 3D Ising Model and ϕ^4 theory live in the same universality class. The concept behind universality lies in the critical point of the Ising Model. At high temperatures the symmetry of the phase is unbroken, therefore $\langle\phi\rangle = 0$, whereas at low temperatures $\langle\phi\rangle \neq 0$ and the symmetry is spontaneously broken. The point at which the phase is broken is the critical point where the phase transition occurs. Equivalently, the $\lambda\phi^4$ model can live in two phases: the broken one if $m^2 > 0$ where the vacuum field expectation value is given by $\langle\phi\rangle = \pm m\sqrt{6/\lambda}$ and occurs at low temperatures and the symmetric phase where the vacuum field expectation value is just $\langle\phi\rangle = 0$.

In [8] and [9], they actually show by considering the spectrum in the critical limit, that implementation of the two models would give results that should match within statistical errors. They are treating non-perturbative states of the ϕ^4 theory in the broken symmetry phase as bound states and they show that they exist by both theoretical explanation and numerical results. This gives the advantage to use the 3D Ising model in the implementation of the ϕ^4 model in Quantum Field Theory.

Chapter 3

Topological Defects

3.1 Basic Ideas behind Topological Defects

Elementary particles as studied and observed so far, have no topological structure. However, studies of the field theory in its non-linear form revealed solitons, that is solitary wave-like excitations of the theory which are actually characterized by their topological structure. Therefore they have the name topological solitons. Their topological structure is determined by a winding number, an integer N, which is the so called topological charge and basically indicates the number of topological solitons that are present. Their energy can be directly interpreted as their mass since, compared to the observed elementary particles the mass of which has an extra factor of $\hbar$, soliton mass does not have this factor, leading it to a much higher value compared to the elementary particles.

In a theory, one usually considers solitons as topological defects which take different forms depending on the dimensions and the theory they are dealing with. These can be kinks, domain walls, vortices, monopoles and many others. The studying of topological solitons is a quite recent area of research. However, a significant amount of researchers in a variety of fields of physics have taken them into account in their theories. Cosmologists are investigating domains walls created in the early universe in addition with cosmic

strings and their effect in the CMB radiation, string theorists consider branes to behave as topological defects and people working in condensed matter started investigating the conductivity in the presence of a topological defect. A very exciting open research topic is that of the confinement in QCD which might be explained by the studies of topological solitons.

Most of the studies of topological solitons are done in systems with phase transitions, since in the spontaneously broken phase it is able for a topological defect to be created and then an order parameter can be constructed based on it. One of the main purposes of most of the previous studies was to measure their mass, their excitation spectrum and similar properties. Before 2009, there were mainly two non-perturbatively ways for constructing an order parameter and getting the properties of a theory out of that.

Firstly, one can consider a creation operator $\langle \mu \rangle$ in the phase where the symmetry is spontaneously broken. This operator was proposed in [10] and [11] by applying Operator Algebra in the two dimensional Ising Model. In [12] they used this operator to find the soliton mass on the $(\lambda\phi^4)_{1+1}$.

The second method of measuring the mass is by considering the free energy of the system. In [13] they explain that when topological defects are present, there is an N winding number and an associated free energy of :

$$F_N = -\ln Z_N \tag{3.1}$$

When $N = 0$, it means that there is no topological defect and thus the free energy goes to zero. Therefore, the mass of it can be found by the free energy difference between the system with a topological defect present ($N = 1$) and with no topological defect ($N = 0$).

Finally, a new method was proposed a couple of years ago by Rajantie and Weir which deals with the correlation functions in the sector where the topological defect is present [1].

In this dissertation the 3D Ising Model is considered and the topological defect that can be created gets the meaning of a domain wall. Thus, the mass of this domain wall can be measured using the methods proposed above. Due to inefficiency of the first, actually only the two latter methods are implemented.

3.2 Topological defect of the 3-dimensional Ising Model and its relation to QCD

Before embarking into the actual procedure that was done for measuring the mass of the topological defect that is present in the model, it is useful to see the importance of its investigation. In Chapter 2 the Ising model and the $\lambda\phi^4$ theory were described. However there was no reasoning why such a large amount of people base their research on them and how these models are related to the topological defects. Every single theoretical physicist has come across the problem of confinement in QCD. This is a research topic that has been investigated for many years without anyone coming up with a final conclusion.

Firstly, 't Hooft published a series of papers in which he explained that the deconfinement and confinement are distinguished by the center symmetry $\mathbb{Z}(N)_c$ of the $SU(N)$ gauge group [14],[15]. Svetitsky-Yaffe conjecture states that a $d+1$ dimensional gauge theory with a second order deconfinement transition and a d dimensional spin model with a $\mathbb{Z}_N$ symmetry belong to the same universality class [16]. From this, it is concluded that the 4-dimensional $SU(2)$ Yang-Mills theory and the 3D Ising Model close to the phase transition, must be in the same universality class. This was in fact shown using Finite Size Scaling in [17]. In Yang-Mills theory, it can be shown that at high temperatures the

center symmetry is spontaneously broken and this corresponds to the deconfining phase. This seems misleading, since according to what it was discussed for the 3D Ising Model it is known that its broken phase occurs at low temperatures. However, it is actually true and this is due to the duality between the 3D Ising Model and the 3D $\mathbb{Z}_2$ gauge model.

In [8] and [9], they argue that the Ising Model in 3 dimensions which obeys a global $\mathbb{Z}_2$ symmetry and the $\mathbb{Z}_2$ gauge model are related by a duality. They have actually shown that the bound states of the 3D Ising Model are mapped to the glueball states of the gauge Model. In [9] they state that this duality is given by a relation between the partition function of the two models as:

$$Z_{gauge}(\beta) \prec Z_{spin}(\tilde{\beta}); \qquad \tilde{\beta} = -\frac{1}{2}\log[\tanh(\beta)] \tag{3.2}$$

So high temperatures of the gauge model correspond to low temperatures of the spin model and vice versa. Thus the broken phase of the Ising model is mapped to the confining phase of the gauge theory. Furthermore, this duality implies that the point at which the phase transition occurs in our spin model corresponds to the point where the deconfinement transition happens.

The order parameter that is used in the Yang-Mills theory comes from the works of Polyakov [18] and Susskind [19] and it is the so called Polyakov loop $P(\vec{x})$ operator. The Polyakov loops at high temperatures have a spontaneously broken phase and they physically describe static quarks when Euclidean action is taken into account. By twisting the boundary conditions of the $SU(2)$ theory on a lattice close to the deconfining transition, i.e. to impose $P(\vec{x})P^{\dagger}(\vec{x} + L\hat{z}) = -1$, a spatial center vortex is created which is called a spatial 't Hooft loop and is dual to the Wilson loop. This is considered to be a topological defect and it turns out to correspond to the spin interface which is created by twisting the boundary conditions of the 3D Ising Model [20], [21].

From what it was discussed above, it is clear that the confinement - deconfinement transition is related to the 3D Ising model. Thus, by measuring the surface tension or the mass of the domain wall that appears after twisting the boundaries of the model will be equivalent to measuring the above properties of the spatial 't Hooft loop created in the 4-dimensional SU(2) Yang-Mills theory. Even more, the latter has a representation of the real scalar field in three-dimensional $\lambda\phi^4$ model which is in the same universality class as the 3D Ising Model, thus it is not surprisingly that the two models have this correspondence. All in all, investigation of the properties, such as the mass or the surface tension and critical exponents of the domain wall appearing in the 3D Ising model after twisting the boundaries, might play a significant role in the understanding of the confinement in QCD. A more detailed analysis of the QCD and the phase transitions between confining and deconfining phases is given in [22].

3.3 Topological defects of the $\lambda\phi^4$ theory in cosmology

Despite all the above, as stated in the introduction, the investigation of the interfaces created as defects in $\lambda\phi^4$ theory have been investigated extensively by cosmologists. Kirzhnits and Linde were the first to propose that the idea of spontaneously symmetry breaking in condensed matter systems applies to elementary particle theories as well [23], [24]. In cosmological models, it is believed that the hot universe went through a phase transition while it was cooling down and symmetry breaking occurred. Dealing with finite-temperature field theory, in [25] and [26], they have shown, that in the effective potential, which has a similar form of the one given in Equation (2.8), the sign of m

is dependent on the temperature i.e.

$$m^2 \simeq (T_c^2 - T^2) \tag{3.3}$$

where the critical temperature at which the phase transition occurs is defined as:

$$T_c = \sqrt{\frac{24}{\lambda}} m. \tag{3.4}$$

At temperatures lower than T_c, m becomes positive and by observing the Lagrangian of the $\lambda\phi^4$ model as given in Equation (2.8), it can be seen that the symmetry is spontaneously broken, i.e. the vacuum expectation value of the field will not be zero anymore but instead it will be able to take one of the two available values. The Hot Big Bang model implies that as the universe was cooled down, temperatures lower than the critical one were reached. Kibble proposed that after it undergoes a phase transition the field can fall into one of the two available vacua without any preference, resulting in the formation of a domain wall [27].

Actually the Kibble Mechanism predicts various topological defects that are present in cosmological models such as cosmic strings, domain walls and monopoles, depending on the nature of the symmetry that is broken and can be found by observing the topology of the model. The manifold in which the fields can fall and the homotopy group associated with it determine the nature of the topological defect. If there are two disconnected parts of the manifold, $\mathcal{M}$, then the first homotopy group $\pi_1(\mathcal{M})$ implies that depending on the number of independent generators of it, different structures of the strings that appear as topological defects can form. Similar arguments apply for the second homotopy group, $\pi_2(\mathcal{M})$, which state that if the latter is non-trivial for the vacuum manifold, $\mathcal{M}$ and the unbroken symmetry group of the theory has a non-trivial fundamental group same as the first homotopy group then topological defects are present in the theory in the form of monopoles.

Domain walls, are associated with the breaking of a discrete symmetry when the manifold, $\mathcal{M}$, consists of two disconnected components, i.e. $\pi_0(\mathcal{M})$ is not trivial. The surface tension of the domain walls plays an important role in the understanding of the structure of the universe since it is believed that if it is large, there should be an impact on the homogeneity of the universe. Therefore, measurements of the surface tension and the mass of the domain wall are of high importance in the understanding of the structure of the universe.

Chapter 4

Measuring the mass of the domain wall

4.1 Twist of the boundaries

In lattice theory, there are non-perturbative ways to measure the mass of a topological defect as stated in the previous chapter. In [28], it was proposed that by twisting the boundaries of a system a dislocation is formed. This dislocation is considered to be a topological defect. In the same paper, they proposed that the surface tension of the dislocation is proportional to the difference between the free energy using twisted and periodic boundary conditions as :

$$\sigma \prec \frac{F_{TW} - F_P}{L^{(d-1)}} \tag{4.1}$$

where σ is the surface tension, F is the free energy, twisted boundary conditions are labeled as TW and periodic boundary conditions as P.

In the case of the 3D Ising Model, when the boundary conditions are twisted in one direction, a domain wall with a string realization is created and can be considered as the

topological defect of the model. When the dislocation that is formed is considered to be square, the surface tension in the case of 3 dimensions is defined as:

$$F_{TW} - F_P = A + \sigma L^2 \tag{4.2}$$

directly from Equation (4.1).

However, the Ising Model, as Hasenbusch showed in his PhD thesis, goes into a roughening transition at a β almost twice as the critical one, that is at around $\beta_r \simeq 0.4074$. So, at inverse temperatures between the β_c and β_r, there is a rough phase of the system. The Equation (4.2) was used in two of his papers in the calculations of the surface tension [29], [30]. However, in [31], they showed that in the roughening regime the two loop expansion gives a correction to the free energy as :

$$F_S = A + \sigma L^2 - \frac{1}{4\sigma L^2} + O\left(\frac{1}{(\sigma L^2)^2}\right). \tag{4.3}$$

Actually, in [30], it was obvious that at inverse temperatures between the critical point and the roughening transition point, the value of $\sigma/(2\beta)$ is almost linear to β - especially at values closer to the critical one. On the other hand, if someone goes at high enough values of β, where the phase is smooth, this value becomes almost constant to β and specifically close to 1. This is indeed in agreement with what it is predicted using the extrapolated low temperature expansion series [32] as :

$$\sigma = 2\beta + \sum_{n=2}^{17} a_n u^n + O(u^{18}) \tag{4.4}$$

where $u = e^{-4\beta}$ and the coefficients a_n were determined by mainly Weeks and Arisue [33], [34].

This is a good point to investigate further how one can calculate the free energy of

the surface, F_s. The domain wall that is formed is presented at temperatures below the critical one, T_c , at which spontaneous symmetry breaking occurs. Then, the free energy of the topological defect can be found by the difference between the free energy of the system with the domain wall , i.e. with twisted boundary conditions and the system without the domain wall, i.e with periodic boundary conditions. By using Equation (3.1), this is just:

$$\Delta F \equiv F_{DW} = F_{TW} - F_P = -\ln \frac{Z_{TW}}{Z_P} \tag{4.5}$$

In a recent paper [35], in which they are dealing with a topological defect in (3+1) dimensions, they are giving with reasoning the exact form of the partition functions of both the twisted and the periodic boundary conditions. The equivalent of those in the model that is considered here are:

$$Z_{TW} = 2Z_0 \left(Z_1 e^{-MT} + \frac{Z_1^3}{3!} e^{-3MT} + ... \right) \tag{4.6}$$

$$Z_P = Z_0 + 2Z_0 \left(\frac{Z_1^2}{2!} e^{-2MT} + ... \right) \tag{4.7}$$

where $Z_1 = \left(ML^2/2\pi T\right)^{1/2}$, T and L are the lattice dimensions in time and spatial direction respectively and M is the mass of the topological defect.

By applying these equations to Equation (4.5), as it can be seen in Appendix A, an equation of the free energy of the topological defect is obtained as following:

$$F_{DW} = MT - \ln 2 - \frac{1}{2} \ln \frac{ML^2}{2\pi T} + O\left(e^{-2MT}\right) \tag{4.8}$$

which takes into account the free translation of the topological defect in time direction, i.e. in one degree of freedom. From this, one can obtain the mass of the domain wall. However, the extra term of the natural logarithm that contains the mass, M, makes its estimation more difficult. As a first approximation, the mass of the domain wall was

taken to be:

$$M \simeq \frac{1}{T}\left(F_{DW} + \ln 2\right) \tag{4.9}$$

but further the mass was found using the full Equation (4.8).

Although this calculation seems straight forward, in Monte Carlo simulations, which are explained in Chapter [5], values of the partition function cannot be calculated directly. Thus, instead of finding the free energy itself, one can calculate derivatives of it with respect to the inverse temperature as following:

$$\begin{aligned} \frac{dF}{d\beta} &= \frac{d}{d\beta}\left(\ln Z_P - \ln Z_{TW}\right) \\ &= \langle \mathcal{H}_{TW} \rangle - \langle \mathcal{H}_P \rangle. \end{aligned} \tag{4.10}$$

Then, to find the mass all that has to be done is to integrate over beta as below:

$$F_{DW} = F_{DW}(\beta_0) + \int_{\beta_0}^{\beta} d\beta' (\langle \mathcal{H}_{TW} \rangle - \langle \mathcal{H}_P \rangle). \tag{4.11}$$

The value of β_0 can be taken to be the critical inverse temperature β_c at which it is known that the domain wall disappears thus there is no interface energy and the term $F_{DW}(\beta_0)$ can be set to zero.

Another approach of this method is to measure the differences in free energy by the finite difference method, i.e. the difference in the free energy between twisted and periodic boundary conditions for small intervals $\Delta\beta$ and then summing over all the differences as following:

$$F = \sum_{i=1}^{N-1} \left(\Delta F_{TW} - \Delta F_{PBC}\right)_i \tag{4.12}$$

where

$$\begin{aligned}\Delta F_i &= F(\beta_i + \Delta\beta_i) - F(\beta_i) \\ &= -\ln \langle \mathrm{e}^{-\Delta\beta\mathcal{H}} \rangle_{\beta_i}\end{aligned} \tag{4.13}$$

Then in principle the free energy difference is given by :

$$\Delta F_i = (F(\beta + \Delta\beta) - F(\beta))_i = -\left(\ln \frac{\langle e^{-\Delta\beta\mathcal{H}} \rangle_{\beta,TW}}{\langle e^{-\Delta\beta\mathcal{H}} \rangle_{\beta,P}} \right)_i \tag{4.14}$$

and the total mass of the topological defect is then found by solving numerically the Equation (4.8) by putting F_{DW} to be the sum over all the finite free energy differences as in Equation(4.12).

4.2 Measuring the mass using correlation functions

As mentioned above, in [1] a new way of measuring the mass of a topological defect was proposed. The main idea was to find a way of measuring the mass using correlation functions. This method has many advantages, the most important of which is that the mass can be found at the desired value of the parameter that is changed by only measuring the correlation function at that particular value. That is, in the 3D Ising Model where β is the parameter that is changed, the mass of the domain wall can be determined at any value of the inverse temperature without having to start from the critical value, β_c.

It is known that the two-point correlation function of an operator is given by

$$C(t_2 - t_1; k) = \langle \mathcal{O}(t_1)\mathcal{O}(t_2) \rangle \tag{4.15}$$

The operators in the above expression, though, are in momentum space so those that imposed in position space, have to be Fourier transformed into momentum space as

following:

$$\mathcal{O}(k) = \int dxdy e^{ikx} e^{iky} \mathcal{O}(x). \tag{4.16}$$

where the above expression depends on the spatial dimensions that are present in the theory.

By inserting the complete set of states and Fourier transforming the fields, the correlation function becomes:

$$C(t_2 - t_1; k) = \sum_{\alpha=0} \langle 0|\mathcal{O}|\alpha\rangle\langle\alpha|\mathcal{O}|0\rangle e^{-i(t_2-t_1)E_\alpha} \tag{4.17}$$

where $|0\rangle$ is the ground state and $|\alpha\rangle$ is the set of states with energy E_α. In order to go into Euclidean space, the wick rotation $t \to -it$ is done and then the final form of the correlation function is given as below:

$$C(t_2 - t_1; k) = \sum_{\alpha=0} \langle 0|\mathcal{O}|\alpha\rangle\langle\alpha|\mathcal{O}|0\rangle e^{-(t_2-t_1)E_\alpha}. \tag{4.18}$$

Focusing, on the theory that is implemented here, the operators that are used are the spins for each lattice point and since the model is considered in a lattice theory, the integral is transformed into a sum. Therefore, the spins in momentum space are given by the following equation:

$$S(t; k) = \sum_{x,y} e^{ikx} e^{iky} S(t, x, y). \tag{4.19}$$

In the presence of the topological defect in this theory, where antiperiodic boundary conditions are imposed, momentum is set to $k = (2n + 1)\pi/L$ in the twisted direction and $k = 2n\pi/L$ in the other two directions. In that case a scalar particle can be absorbed and re-emerged by the defect if it hits it while it is traveling. Actually, in the case of this dissertation, the particle hits the domain wall giving it a momentum of k and thus

causing it to move until at time t the particle is re-emerged and due to conservation of momentum the wall loses momentum of value $-k$. Consequently, the correlation function for the specific case becomes:

$$C(t;k) = \sum_{\alpha=1}^{\infty} \frac{\langle 0|S(0;k)|\alpha\rangle\langle\alpha|S(t;-k)|0\rangle}{\langle 0|0\rangle} e^{-t(E_\alpha - E_0)} \tag{4.20}$$

where $E_0 = M$ as a result of defining the $|\alpha\rangle$ states relative to the ground state.

All states $|\alpha\rangle$ have a total momentum of k, due to conservation of momentum. The lightest corresponds to the topological defect and the others to the excited states of the latter or states consisting both of the domain wall and the boson. In [36] they actually claim that for $t \geq 1/2M$ the gap between the first state, which corresponds to the domain wall and the rest states is large, resulting into suppression of the latter and thus the state of the topological defect becomes dominant.

Also due to periodic boundary conditions that are imposed in time direction, traveling forward in time until time T is reached, is equivalent of going back to time 0. In [1] it is shown that the correlation function takes the following form:

$$C(t;k) \prec \exp\left(-(E_k - E_0)\frac{t(T-t)}{T}\right) \equiv \exp\left(-\frac{Et(T-t)}{T}\right) \tag{4.21}$$

where T is the lattice dimension in time direction, E_0 equals the mass M and the energy, E_k, is given by:

$$E_k = \sqrt{k^2 + M^2}. \tag{4.22}$$

Hence, the total mass is found by:

$$M = \frac{k^2 - E^2}{2E}. \tag{4.23}$$

It is also useful to see the behaviour of the correlation functions in the case of periodic boundary conditions where no topological defect is present. A scalar particle is created at time 0 and travels until it is detected in time t. The correlation of this particle that is allowed to travel free is given by:

$$C(t;k) \prec e^{-Et} + e^{-E(T-t)} \tag{4.24}$$

taking into account that traveling forward in time is like going back to time $t = 0$ since periodic boundary conditions are imposed. Also, due to the specific boundary conditions, momentum can be set to $k = 0$ and thus the energy $E = \sqrt{k^2 + m^2}$ reduces to just $E = m$. In fact, the mass is equivalent to the inverse correlation length which is defined as:

$$\xi \prec |T - T_c|^{-\nu} \tag{4.25}$$

where ν is a critical exponent which is universal. So, the correlation length is expected to be independent of the lattice size but to depend on the temperature.

In fact the contribution due to the free scalar particle, which is given by Equation (4.24), has to be taken into account in the correlation function when the topological defect is present. So the final form of the two-point function is given by:

$$C(t;k) = A_1 \exp\left(-\frac{Et(T-t)}{T}\right) + A_2\left(e^{-mt} + e^{-m(T-t)}\right) \tag{4.26}$$

In principle, this method has the advantage that one only needs to deal with the twisted boundary conditions and results for the periodic boundary conditions case are not needed. However, when computing the mass using this method, the program can be checked to be

working by imposing periodic boundary conditions. In that case the correlation function will have the form of Equation(4.24) and values of m can be obtained. As discussed above, this is equivalent to the inverse correlation length and values of it can be found in literature. Also, its value can be used to make easier the fit of Equation (4.26) to the data that our program obtains for the correlation with anti-periodic boundary conditions. Therefore, the procedure of finding the mass of the domain wall is simplified.

Chapter 5

Monte Carlo Simulations

5.1 Introducing the idea of Monte Carlo Simulations

The idea of Monte Carlo Simulations was first introduced by Neumann, Ulam and Metropolis who came up with the idea that by generating pseudorandom numbers for a long time the desired result can be reached. Since then, Monte Carlo simulations have become very popular and they have been used to solve different problems both in Physics and Mathematics.

The Ising Model can be solved using the Mean Field Theory. However, it becomes very complicated in 3 dimensions, so the introduction of a different approach in order to find solutions to the model was necessary. After the idea of simulating the Ising Model using Monte Carlo simulations was introduced, the values of observables found both analytically and by numerical simulations, for the case of D=1 and D=2, were in perfect match.

The Monte Carlo Simulations process is based on the generation of a Markov chain, that is a memoryless sequence of spin configurations. The initial configuration is chosen to be random and each of the rest configurations is generated from its previous one. The

generation of a new spin configuration, s', from a current configuration, s, is given by the transition probability $\mathcal{T}(s \to s')$ which satisfies:

$$\sum_{s'} \mathcal{T}(s \to s') \ = 1 \tag{5.1}$$

After a sufficient number of iterations of Monte Carlo steps, since every spin configuration is generated by only its previous one, the final spin configuration becomes independent of the first one, which was chosen randomly. At this point, it is said that the system has reached equilibrium and the probabilities of the spin configurations follow a Boltzmann distribution.

In order to implement Monte Carlo simulations there are a lot of algorithms which are based on the Markov process. However, to ensure that the algorithms are generating the correct system and they work properly, there are two conditions that are needed to be satisfied: *ergodicity* and *detailed balance*.

By ergodicity it is meant that in a Markov process it is possible, in principle, to reach any other configuration from the current one. By this, it is ensured that all spin configurations are included in the calculations and thus they are generated by their correct Boltzmann probabilities. However, in order for the spin configurations to follow the Boltzmann probability distribution and not any other distribution, the algorithm must obey the detailed balance conditions. This condition implies that the transition probability rate in and out of a configuration must be equal, i.e. satisfy the following equation:

$$\mathcal{T}(s' \to s)\mathcal{P}(s') = \mathcal{T}(s \to s')\mathcal{P}(s) \tag{5.2}$$

where $\mathcal{P}(s)$ is the Boltzmann probability given by Equation (2.2). Combining Equations (2.2), (5.1) and (5.2) it is clear by Equation (5.3) that the transition probability rate

depends only on the difference in energy:

$$\frac{\mathcal{T}(s \to s')}{\mathcal{T}(s' \to s)} = \frac{\mathcal{P}(s')}{\mathcal{P}(s)} = e^{-\beta(\mathcal{H}(s')-\mathcal{H}(s))} = e^{-\beta\Delta\mathcal{H}}. \tag{5.3}$$

Another important property of this condition is that it implies that the process is reversible. Real systems must have detailed balance symmetry since time-reversal violation is not permitted. Thus, ensuring that the algorithm of our program satisfies this condition implies that it would give results similar to those of systems in the real world.

5.2 The Metropolis Algorithm

The most well known Monte Carlo algorithm is the Metropolis algorithm proposed in 1953 by Nicholas Metropolis et al. in [37]. In this algorithm the transition probabilities depend on the difference in the energy between the old and the new spin configuration. A selection of probabilities $g(s \to s')$ is made which gives the probability of selecting each of the spin states. Assuming that all spins have the same probability to be selected this is just $1/N$. Therefore the transition rate as discussed in Section 5.1 and using Equation (5.3) is given by:

$$\frac{\mathcal{T}(s \to s')}{\mathcal{T}(s' \to s)} = \frac{g(s \to s')}{g(s' \to s)} \frac{\mathcal{P}(s')}{\mathcal{P}(s)} = e^{-\beta\Delta\mathcal{H}} \tag{5.4}$$

In fact the Metropolis Algorithm consists of three basic steps:

1. Choose a random spin state and flip the sign.

2. Calculate the difference in the energy $\Delta\mathcal{H}$ of the system.

3. If $\Delta\mathcal{H} < 0$ then accept the flip of the sign, otherwise accept the flip of the sign with a probability of $e^{-\beta\Delta\mathcal{H}}$.

5.3 Equilibration

In order to get accurate results, we should ensure that the system has reached equilibrium before taking any actual measurements. To achieve this, the equilibration time should be found, i.e. the number of Monte Carlo steps needed for the system to reach equilibrium. This is also referred as thermalization process.

This equilibration time is found by letting the system do a number of Monte Carlo steps and at each step measure the total magnetization or total energy of the system. When these values appear to be roughly constant then it is said that the system has reached equilibrium and it is safe to take actual measurements. A sample of the way the equilibration time was measured, is shown in Figure 5.1, in which the behaviour of the total energy and magnetization versus time (Monte Carlo steps) for two different cubic lattices N=14, 18 is shown. It is clear that at low temperatures the equilibration time can be estimated easily. However, at T close to T_c there are significant fluctuations that increase the error in the measurements. This indicates that a large number of Monte Carlo steps is needed to be performed after thermalization in order to get more accurate results. Also, it is easily observed that the equilibration time depends on the lattice size, i.e. the bigger the lattice the higher the number of Monte Carlo steps needed until equilibrium is reached.

However, one might think that the system might not be in its global minimum but instead it might be stuck in a local minimum for a while, resulting to give us a constant value of the total energy or magnetization over time. A way to ensure that the estimated equilibration time is the correct one was proposed in [38]. In that book, they performed the thermalization process two times starting at different temperatures each time. Firstly, they started from $T = 0$ where all spins are aligned and they repeated it starting at a high temperature where the configuration of the system is random. The equilibration time using both starting temperatures must be the same if we are reaching the global

minimum. In Figure 5.2 we can see a comparison of the two methods.

L=14

(a) Total Magnetization

(b) Total Energy

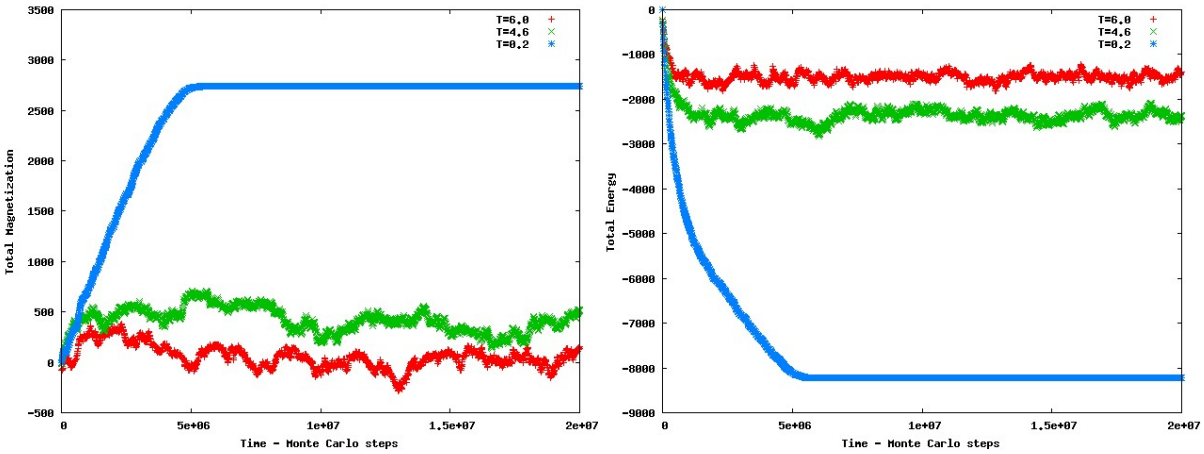

L=18

(c) Total Magnetization

(d) Total Energy

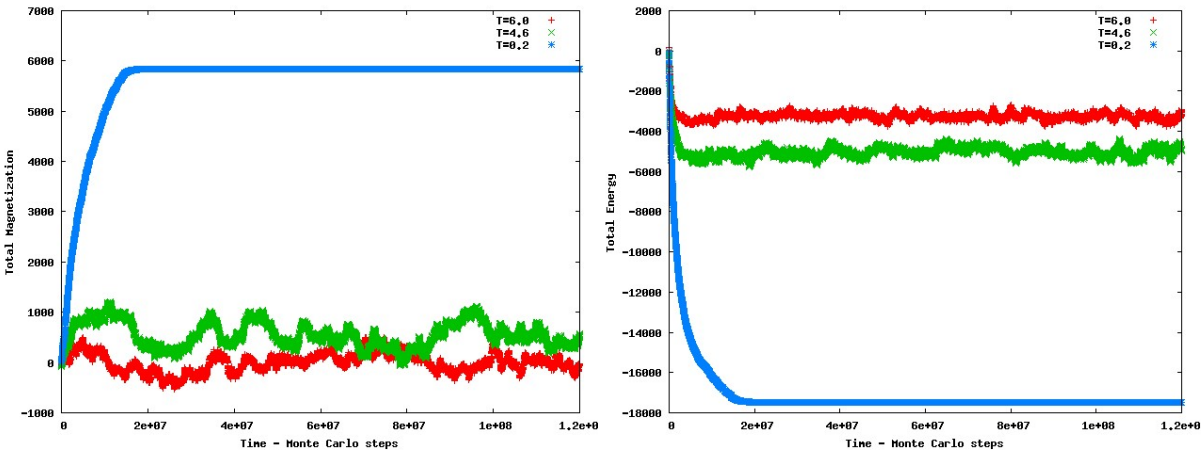

Figure 5.1: Plots of the Absolute Magnetization and Total Energy across Monte Carlo steps for L = 14 and L = 18. These measurements were taken for $T = 6.0$, $T = 4.6$ and $T = 0.2$ As a safe value for the thermalization steps we took M = 30000000 for L=14 and M = 120000000 for L=20.

L=14

(a) Total Magnetization **(b)** Total Energy

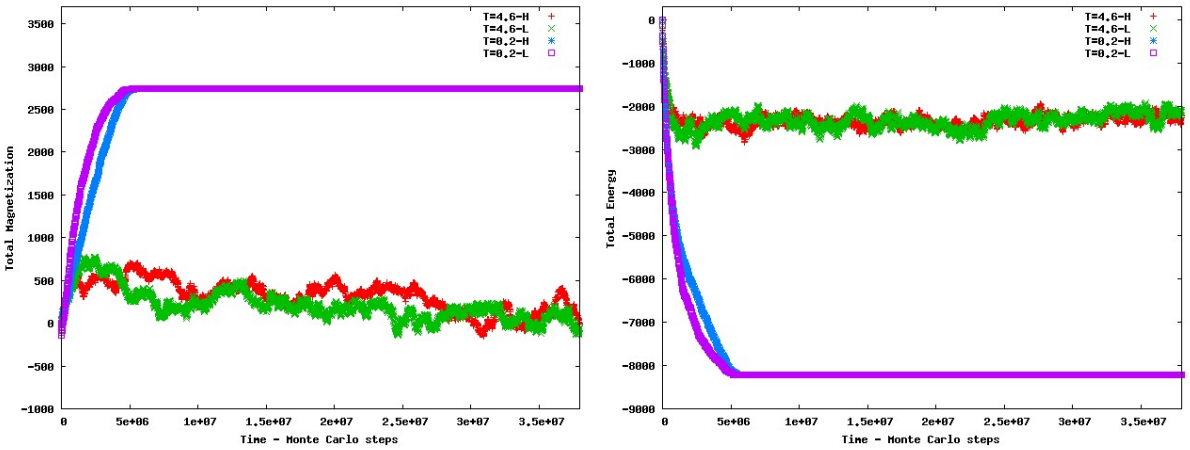

L=18

(c) Total Magnetization **(d)** Total Energy

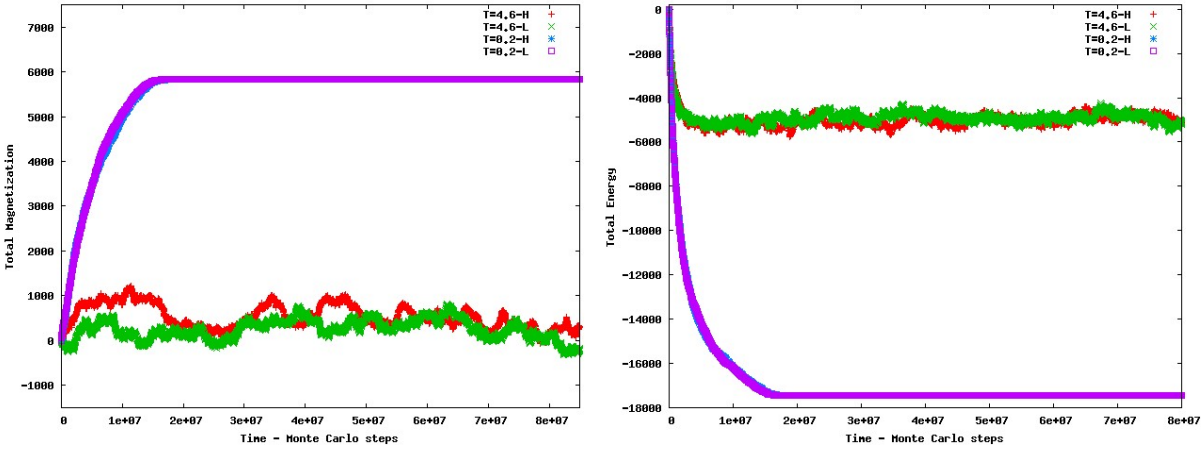

Figure 5.2: Plots of the Absolute Magnetization and Total Energy across Monte Carlo steps for L = 14 and L = 18. They were plotted using data starting from $T = 6.0$ and going to $T = 0.1$ and vice versa. The equilibration time agrees with both methods and we can say that the system has reached its global minimum.

5.4 Error analysis

Monte Carlo simulations is a statistical way of determining values of observables, therefore it contains large statistical errors. There is a variety of factors that contribute in these errors.

Firstly, the finite lattice effect must be taken into account. From several tests that were done, it was clear that for a higher lattice size we could get more accurate results for the second order phase transitions. However, this has a cost in the computational time required, therefore in this dissertation the lattice dimensions that were used were in the range of 14^3 and 20^3. There is still a small contribution in the error due to finite lattice-effect but these lattice sizes were the best that could be used taking into account the amount of time available for the completion of this dissertation.

Furthermore, the number of measurements taken leads to an additional error. Since we are dealing with a purely statistical model, the higher the number of measurements the lower the statistical error. In the whole dissertation the number of measurements taken was dependent on what it was measured such that the computational time for one run of every program used would not exceed 24 hours. There was an attempt to increase the number of measurements as much as possible in order to reduce significantly its error contribution. This was done especially in the calculation of the mass using the first method proposed in Section 4.1 in which, for accurate results, $\Delta\beta$ had to be taken to be really small and the number of Monte Carlo steps to be very large.

However, the most important error in Monte Carlo simulations arises from the autocorrelation function. As it was seen in Section 5.1, we are dealing with a Markov-chain in which all the configurations are statistically dependent since they are generated by the previous ones. Therefore, it is said that they are autocorrelated. In order to estimate the autocorrelation time the autocorrelation function is used which is defined as following:

$$C(t) = \frac{1}{N-1} \sum_{\Delta t=1}^{N} [(\mathcal{O}(t) - \langle \mathcal{O} \rangle) - (\mathcal{O}(t+\Delta t) - \langle \mathcal{O} \rangle)] \prec e^{-t/\tau} \tag{5.5}$$

The procedure that was followed was to plot the autocorrelation function $\frac{C(t)}{C(0)}$ versus t for every temperature and then estimate the time at which $C(t)/C(0) \simeq 1/e$. In Figure

5.3, an example of what it was measured for every temperature can be seen.

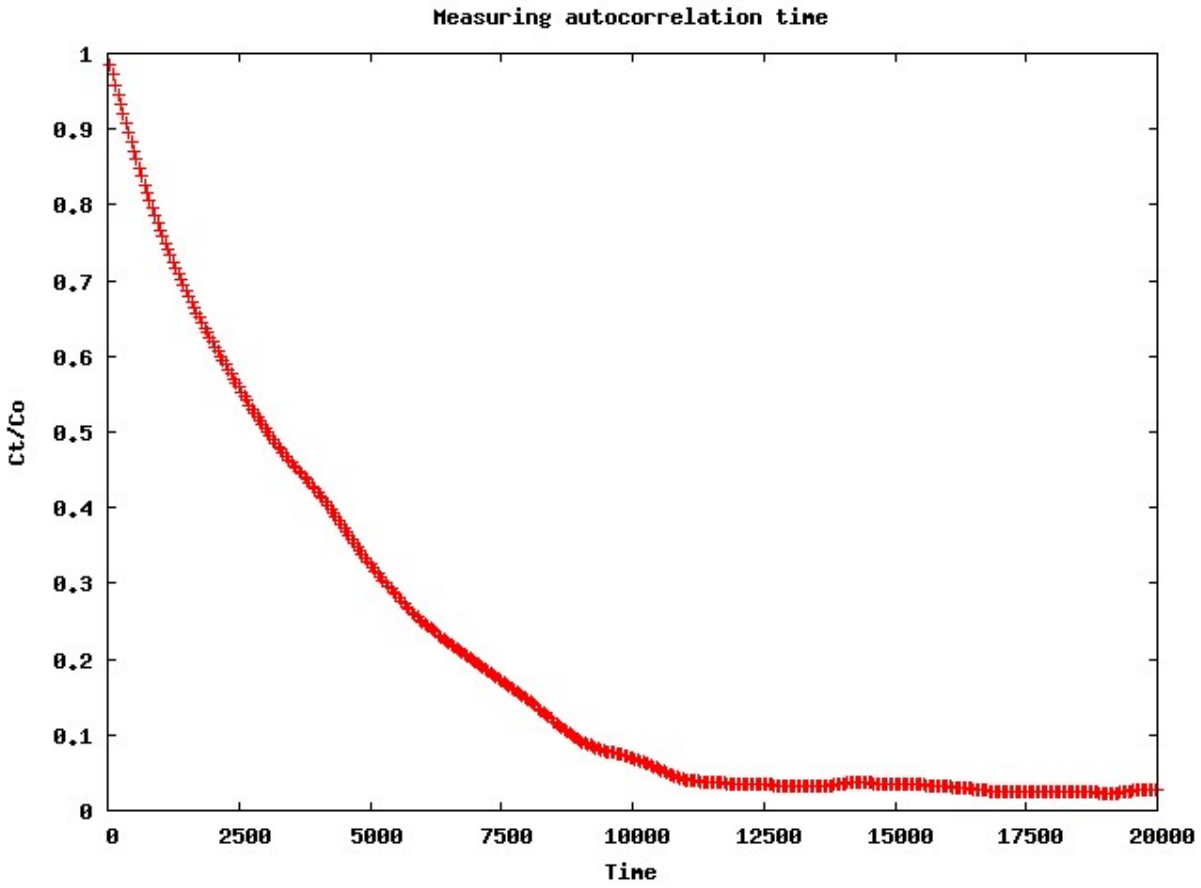

Figure 5.3: The normalized autocorrelation function across time. The value of t at which $C(t)/C(0) \prec 1/e$ is considered to be the autocorrelation time τ.

After finding the autocorrelation time the error of the observable is given by :

$$\Delta\mathcal{O} = \sqrt{\frac{\langle\mathcal{O}^2\rangle - \langle\mathcal{O}\rangle^2}{N-1}2\tau}. \tag{5.6}$$

as shown in [39]. This works well for temperatures below or above the critical temperature. However, in [40] it was stated that $\tau \prec \xi^z$, where z is a dynamic exponent and ξ is the autocorrelation length. The latter diverges as it comes closer to the second order phase transition. In the case of Metropolis Algorithm, after many simulations, its exponent was estimated to be $z \approx 2$ and thus τ diverges at $T \simeq T_c$ failing to give accurate values of observables close to the critical temperature.

Chapter 6

Results of the 3D Ising Model using Periodic Boundary Conditions

The main target of this dissertation is to measure the mass of a domain wall that is created by twisting the boundaries. More about it was explained in Section 4.1. To do this, a program was written, in which the 3D Ising Model was simulated by imposing twisted boundary conditions in one direction. However, in order to ensure that the program that was used was correct, a test using periodic boundary conditions was done. In this chapter, the way of implementing the 3D Ising Model using Monte Carlo simulations in FORTRAN programming language, graphical results of the measured observables and a way of estimating the critical temperature are presented. Also, the program used is given in Appendix C.1.

6.1 Method and Conventions

To find values of observables such as the magnetization and internal energy of the system, the 3D Ising Model was simulated using the Metropolis Algorithm. As it was discussed in Section 5.2 this is an algorithm that obeys ergodicity and detailed balance and gives quite accurate results. Of course there are more efficient algorithms such as Swednsen Wang

Cluster Algorithm, Wolff Cluster Algorithm or Hybrid Metropolis Algorithm which give even more accurate results and they reduce the computational time. However, for the purpose and the length of this dissertation it was decided that the Metropolis Algorithm is sufficient.

Firstly, a few conventions that were used in the code are listed below. The interaction energy, J, was set to 1 for our convenience as well as the Boltzmann constant, k, such that $\beta = 1/T$. The parameter that was changed throughout the program was the temperature and the results that are presented here were obtained by taking measurements from high to low temperatures and thus the initial configuration was chosen to be random. Despite this, the program was tested and it gives similar results implementing it either from high to low temperatures or vice versa.

For the periodic boundary conditions, it was ensured that the first and the $(N+1)^{th}$ spin in every lattice site are the same, so that if one wants to visualize the cubic lattice embedded in a manifold, it would give a 3-torus, $\mathbb{T}^3$.

6.2 Magnetization and Energy of the system

For each temperature there was a number of N Monte Carlo steps of which the first M were used for equilibration. After equilibration, measurements of the energy, the magnetization and their squares were taken every 1500 Monte Carlo steps. From these, their average values could be recorded for every temperature.

Following, in this section, there are graphs of the model for the periodic boundary conditions presenting the absolute value of the average magnetization and the average energy per lattice point. In Figures 6.1a and 6.1b the magnetization for two different lattice

sizes is plotted across the temperature. The behaviour of these graphs is the expected one since magnetization is close to 0 at high T, where the system is highly disordered and goes to 1 at low T, at which the system is oriented. In between, going from 0 to 1 there is a discontinuous phase, which shows that the system goes through a second order phase transition. From this, it can be seen that the transition temperature should be around $T_c \simeq 4.5$. Also, it can be noticed that the errors of the values corresponding to temperatures closer to the critical one are higher than the others and this is due to the autocorrelation time which diverges at the phase transition.

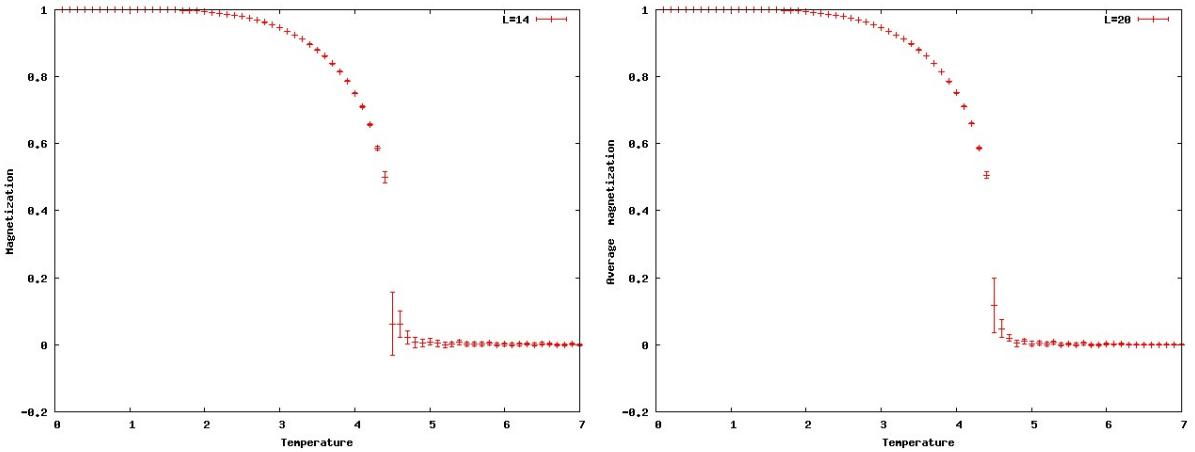

(a) L = 14 **(b)** L = 20

Figure 6.1: Plots of the Average Magnetization across Temperature for L = 14 and L = 20. The phase transition appears to occur at around $T \simeq 4.5$. At this point the error appears to be higher than the others due to the divergence of the autocorrelation time at the critical temperature.

Moreover, in Figure 6.2 the energy per site of the lattice is shown and its behaviour is the expected one: the energy is lower at lower temperatures where the system is ordered, that is the spins are aligned. Since a three-dimensional spin model is taken into account, each spin has six neighbouring spins. However, to avoid over-counting in the calculations of the energy, either it has to be divided by two or only the three spins that are next to the current spin in the forward direction should be considered. That is, if we are dealing with the spin $S(x, y, z)$ we have to take its interaction with the spins

$S(x+1,y,z), S(x,y+1,z)$ and $S(x,y,z+1)$. So, in the specific model, considering the definition of the energy given by Equation(2.5), when all spins are parallel, the interaction energy of every spin will be $\mathcal{H} = -3$. This is indeed the case as shown in Figures 6.2a and 6.2b.

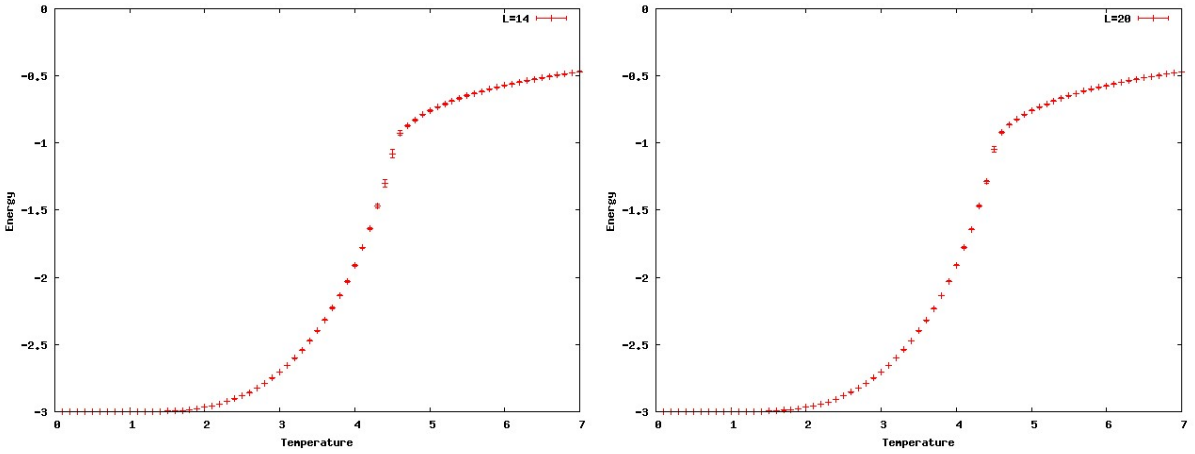

(a) L = 14 **(b)** L = 20

Figure 6.2: Plots of the Energy per lattice space across Temperature for L = 14 and L = 20. The discontinuous phase is obvious to be around T = 4.5 which is considered as the critical temperature.

6.3 Magnetic susceptibility and Specific Heat

For a better understanding of the phase transitions, the specific heat and the magnetic susceptibility were also studied. These observables are given by the values that were already measured and they have a peak at the temperature at which the phase transition occurs. Specifically the specific heat is given as below:

$$\begin{aligned} C_v &= \frac{\partial \langle \mathcal{H} \rangle}{\partial T} = \beta^2 \frac{\partial \langle \mathcal{H} \rangle}{\partial \beta} = \beta^2 \frac{\partial^2 \ln Z}{\partial \beta^2} = \beta^2 \frac{\partial}{\partial \beta} \left(\frac{1}{z} \frac{\partial Z}{\partial \beta} \right) \\ &= \beta^2 \left[\frac{1}{Z} \frac{\partial^2 Z}{\partial \beta^2} - \frac{1}{Z^2} \left(\frac{\partial Z}{\partial \beta} \right)^2 \right] \\ &= \beta^2 \left(\langle \mathcal{H}^2 \rangle - \langle \mathcal{H} \rangle^2 \right) \end{aligned} \tag{6.1}$$

and similarly the magnetic susceptibility is given by:

$$\chi = \beta \left(\left\langle M^2 \right\rangle - \left\langle M \right\rangle^2 \right). \tag{6.2}$$

An idea of how χ and C_v versus temperature look like is given in Figures 6.3 and 6.4.

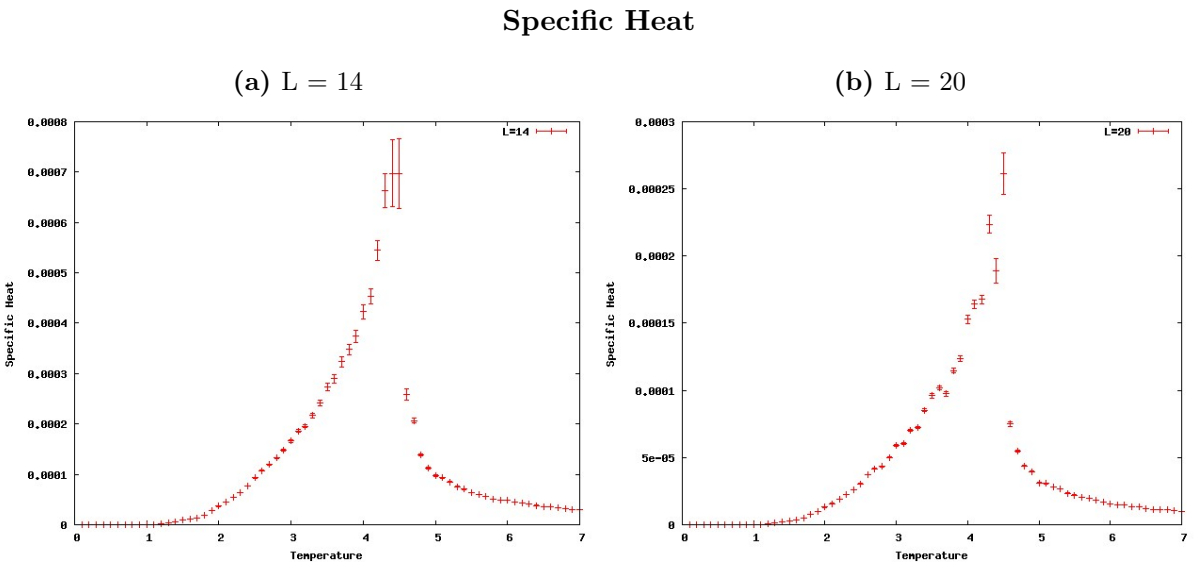

Figure 6.3: Plots of the Specific Heat across the temperature for L = 14 and L = 20. The phase transition is clear to be at around T = 4.5

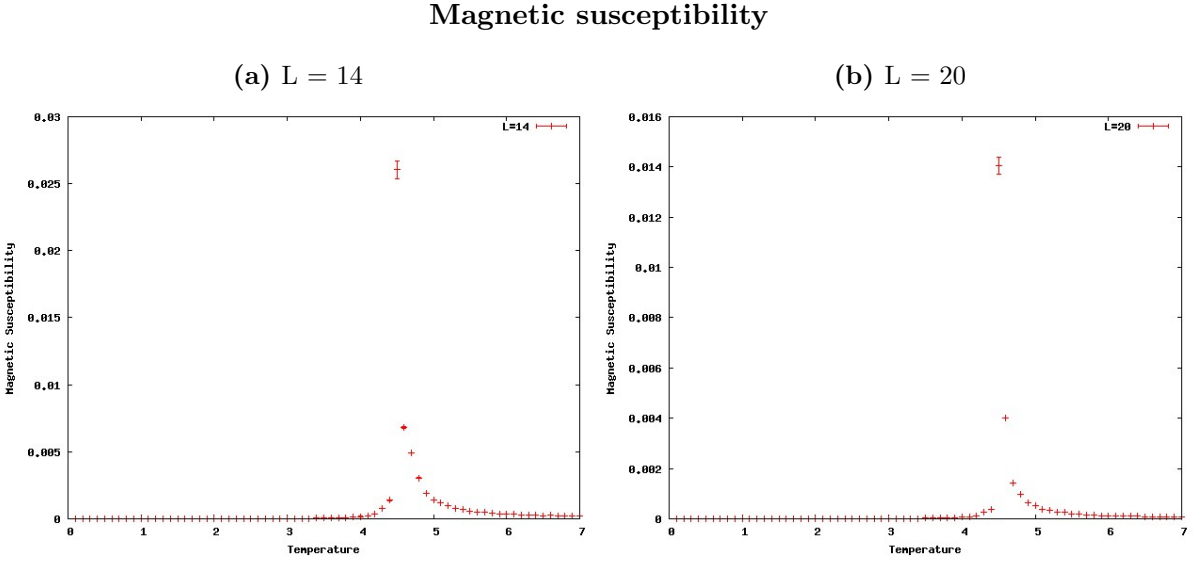

Figure 6.4: Plots of the Magnetic Susceptibility across Temperature for L = 14 and L = 20. Here, it is much clearer that the phase transition occurs at around T=4.5.

6.4 Estimating the critical temperature T_c

From what it is discussed above in this chapter, it is clear that there is a phase transition and magnetization is an order parameter. Therefore, it can be used in finding critical exponents and the bulk transition temperature T_c.

A way to measure them was proposed by Binder in [41] in which he deals with dimensionless quantities. He shows that by finding the 'Binder Cumulant' or Binder ratio for different lattice sizes, one can find the temperature at which the curves cross. The Binder Cumulant is defined as:

$$U_L = 1 - \frac{\langle M^4 \rangle}{3 \langle M^2 \rangle^2} \tag{6.3}$$

Since the quantity is dimensionless, this temperature is considered to be the critical temperature T_c.

In the simulations presented in this work, U_L was computed using a program written again in FORTRAN which had the same structure as the program used for the results in Sections 6.2 and 6.3. The main differences were that records of the energy were not taken and instead quantities such as M^4 and M^8 were calculated. The latter was needed in finding the error δU_L which was estimated to be:

$$\delta U_L = U_L \sqrt{\left(\frac{\delta \langle M^4 \rangle}{\langle M^4 \rangle} \right)^2 + 4 \left(\frac{\delta \langle M^2 \rangle}{\langle M^2 \rangle} \right)^2} \tag{6.4}$$

where $\delta \langle M^4 \rangle$ and $\delta \langle M^2 \rangle$ were found using the standard deviation.

However, since the program run for a long time doing many Monte Carlo iterations, the contribution in the error given by Equation (6.4) was negligible. Therefore, the error bars are not visible on the graph in Figure 6.5 and the error of the critical tempera-

ture was found by estimating the difference between the two nearest points close to the crossing of the plots. This value was estimated to be:

$$\boxed{T_c = 4.51 \pm 0.01} \tag{6.5}$$

or equivalently:

$$\boxed{\beta_c = 0.2217 \pm 0.0005} \tag{6.6}$$

which is in the range of the values estimated in previous works by many researchers who used different approaches[42],[43],[44].

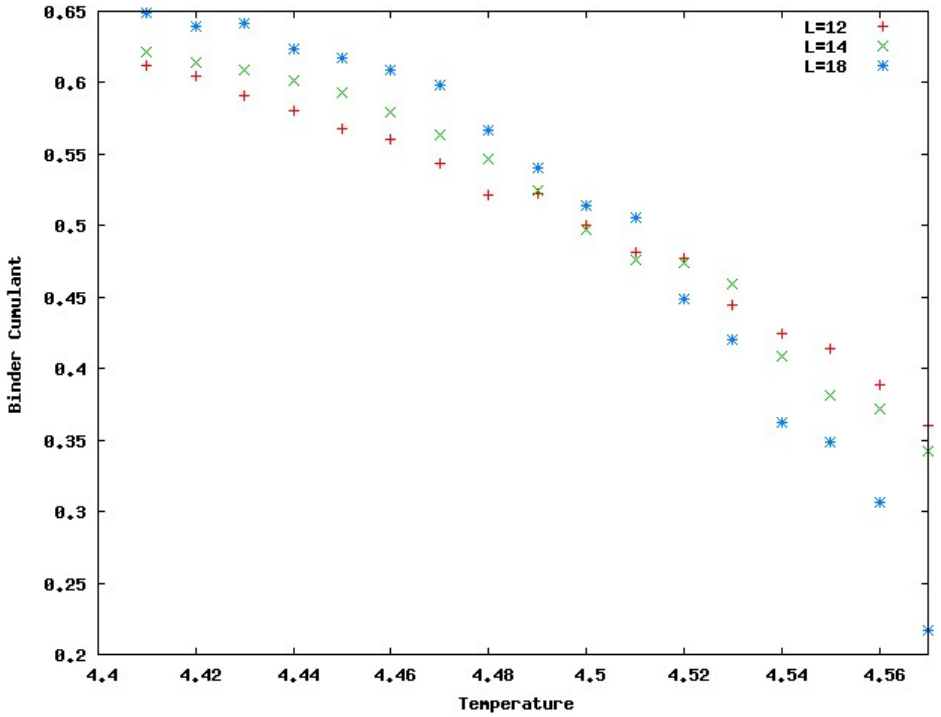

Figure 6.5: The Binder Cumulant for the 3D Ising Model. The temperature, at which the lines cross, is the critical temperature. The three different curves correspond to L=12, L=14 and L=18 and they meet at around $T_c = 4.51 \pm 0.01$.

Chapter 7

Results of the mass of the topological defect

7.1 Results using finite free energy differences

As discussed in Chapter 4, the mass of the domain wall was found using two different methods. In the first method, finite energy differences were calculated and from those the mass could be extracted. To ensure that the statistical error was minimized and the interval $\Delta\beta$ was small enough to give accurate results, the method used in [45] was applied, where the expectation value of the free energy is calculated using two different ways :

$$f_1 = -\ln\langle e^{-\Delta\beta\mathcal{H}}\rangle_{\beta_1} \text{ and } f_2 = \ln\langle e^{\Delta\beta\mathcal{H}}\rangle_{\beta_2} \tag{7.1}$$

Then, Equation (4.14) becomes :

$$\Delta F_i = \frac{1}{2}\left[f_{1,TW} + f_{2,TW} - f_{1,P} - f_{2,P}\right]. \tag{7.2}$$

The error in each f_i, δf_i, can be found using standard error analysis since the expectation value of the exponential of the energy is just the average over a number of measurements. Thus, the associated error in the mass difference is given by:

$$\delta(\Delta F_i) = \frac{1}{2}\sqrt{\left[\delta f_{1,TW}^2 + \delta f_{2,TW}^2 + \delta f_{1,P}^2 + \delta f_{2,P}^2 + (f_{1,TW} - f_{2,TW})^2 + (f_{1,P} - f_{2,P})^2\right]} \tag{7.3}$$

The difference in free energies, as given in Equation (7.2), was measured for different lattice sizes, starting at the critical point $\beta \simeq 0.22165$ where the domain wall vanishes. Actually measurements were taken for cubic lattices of size $14^3, 16^3, 18^3$ and 20^3 for inverse temperatures ranging between 0.225 and 0.23. The free energy of the topological defect, calculated using the above method, is shown in Figure 7.1 where the results for different temperatures and different lattice sizes are plotted. As expected, the free energy grows with the inverse temperature and it is highly dependent on the lattice size, especially as one goes deeper into the broken phase.

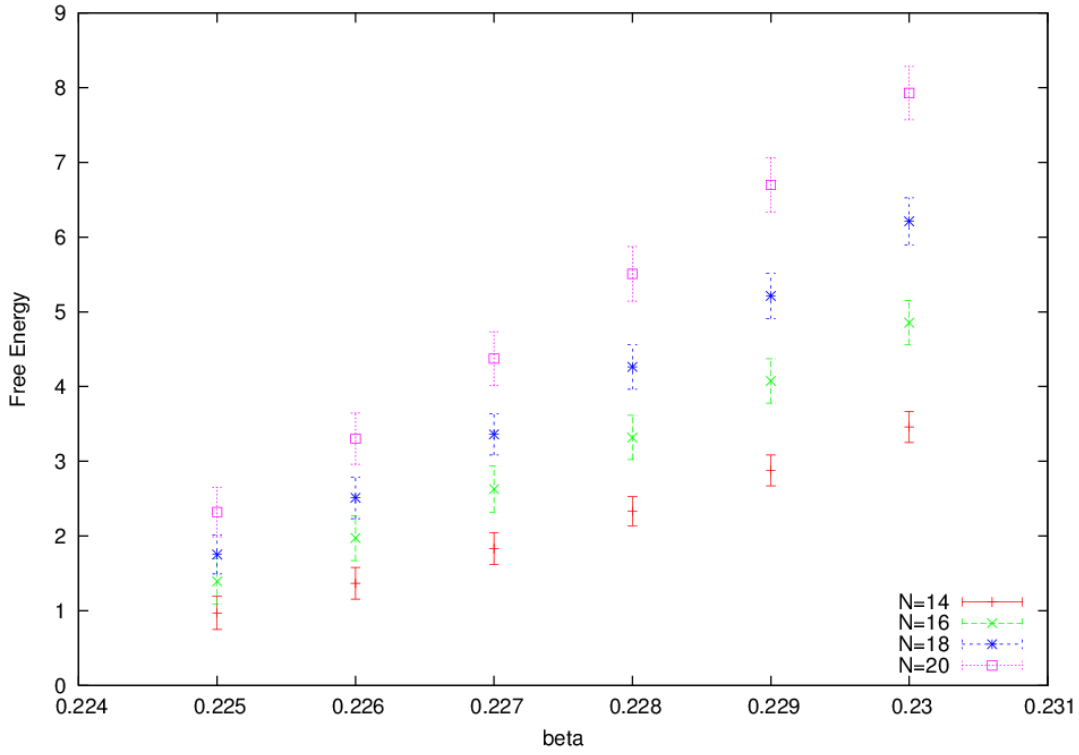

Figure 7.1: The free energy of the topological defect for lattice sizes of $14^3, 16^3, 18^3$ and 20^3. The lattice effect is clear since for higher lattice sizes the free energy increases. Also the higher the inverse temperature, the higher the free energy of the defect.

It is also noticeable that the errors, especially at lower inverse-temperatures, are very

large, reaching even values of 22%. As discussed in Section 5.4, this is mainly due to the autocorrelation time which is dominant close to the critical point.

In order to find the mass, as a first approximation, we applied Equation (4.9), which involved a trivial calculation. However, especially at small values of β , the factor of $\ln(ML^2/2\pi T)$ must have a significant effect so the mass was found using the full expression of the free energy difference - Equation (4.8) - up to and including corrections of the order of (e^{-MT}). This was solved with respect to M using numerical methods and in fact the assumption that the extra term that was not included in the first approximation does indeed contribute in the mass calculations was confirmed. This can be seen in Figures 7.2a and 7.2b where plots of the mass using the first approximation and the full expression for two different lattice sizes are presented.

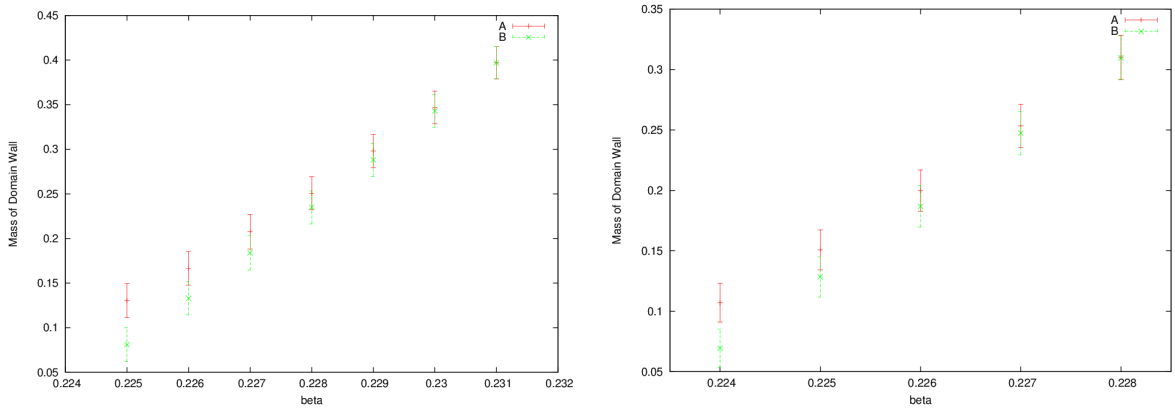

(a) N=16 **(b)** N=20

Figure 7.2: Mass measured using both the first approximation according to Eq. (4.9) and the full Equation (4.8). Values of A were obtained using the former and values of B using the latter in both graphs. The corrections that are taken into account, as shown in B, are significant at low inverse temperatures and especially at smaller lattice sizes.

The method for finding the free energy of the topological defect that was used in this chapter had already been applied for the same model by mainly Caselle and Hasenbusch in a series of papers [29], [30], [31], [46]. The mass of the defect was estimated in none of these papers, however results of the surface tension of the 3-dimensional Ising Model

were published. In fact, in [29] and [30], they used Equation (4.2), from which σ was estimated and in [31] they used the full Equation (4.3). Values of the measured surface tension for the temperatures that are used in this work are given only in [30].

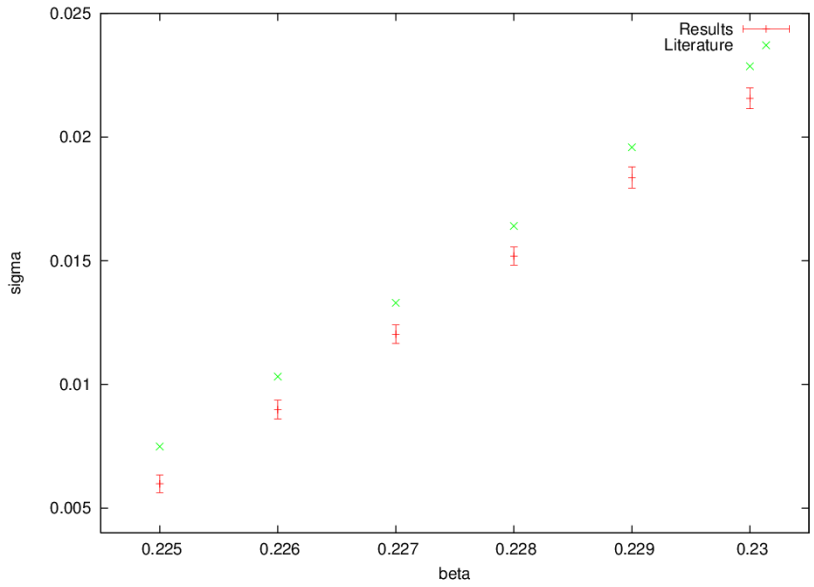

Figure 7.3: Surface tension measured by making a fit of the data to Eq. (4.3). The results are comparable to those found in literature taking into account the different approach that was used in literature.

The data of the free energy of the defect for the four different lattice sizes that were used (14,16,18,20) were fitted to Equation (4.3) and from that the surface tension was found for every temperature. The results could be compared with those given in [30] taking into account that in that paper they did not include the corrections of order $(1/\sigma L^2)$ but instead, they included a term of $\ln T$ in the free energy to take into account the entropy due to the free translation of the surface in one direction. The comparison can be seen in Figure 7.3, where it seems that there is a general agreement of the values estimated in this dissertation with those found in literature.

In addition, as stated in Section 4.1, the quantity $\sigma/2\beta$ should be linear to beta. To

confirm that the estimated values follow this trend, a graph of $\sigma/2\beta$ versus β was plotted (Figure 7.4) and a straight line was fitted to the data points. From the fitting the value of R-squared was found to be almost 1 which shows that the relation between the two plotted values is indeed linear. Also, the values of the gradient of both the results of this work and those of [30] were found to be in agreement within an error of 0.3%.

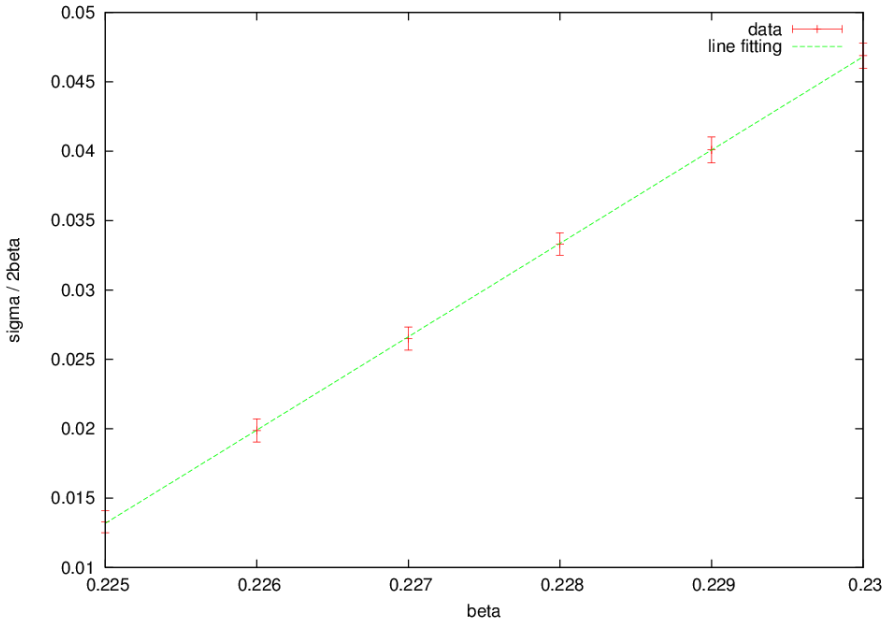

Figure 7.4: The value $\sigma/2\beta$ plotted versus β. It gives a linear plot as expected from the low temperature series expansion [32].

7.2 Results using correlation functions

The new method which is explained in Section 4.2 was applied here in order to estimate the mass of the topological defect, M. A Program in FORTRAN 95 was written which also involves Monte Carlo Simulations (Appendix C.2). However, instead of measuring free energies for twisted and periodic boundary conditions starting from the critical point, the program was chosen to run at a particular inverse temperature, that could be given by the user and find the correlation function at that particular value imposing twisted

boundary conditions.

Even though, for the estimation of the mass of the domain wall, only twisted boundary conditions are needed, in this dissertation periodic boundary conditions were also used from which the mass of the scalar particle could be measured. Basically, the investigation of the two cases of the boundary conditions was done using the same program with only two differences. Firstly, the boundary conditions in Monte Carlo Simulations were fixed appropriately so that if periodic boundary conditions were needed, the spins at point S_i and S_{i+L} were the same whereas if twisted boundary conditions were needed, the above spins were chosen to be opposite. The other difference that was made was in the fixed value of k, the momentum that was used in the Fourier transform of the field or the spin in this case. Specifically, k was chosen to be zero for the periodic boundary conditions and π/L for the twisted boundary conditions. The value of k was kept fixed throughout the program and thus the mass could be extracted from the correlation function.

An idea of what it was seen when periodic boundary conditions were imposed can be seen in Figure 7.5. This is the expected behaviour of the correlation function with periodic boundary conditions since by Equation (4.24) it is clear that it should be symmetric. Also, it is expected that a plateau should be present where the correlation function goes to zero. The plateau is more apparent at larger lattice size and at temperatures away from the critical point.

By fitting the data to Equation (4.24) the energy of the scalar particle can be found. In the process of fitting the data to the equation, three points from each end were excluded to avoid including the short-range behaviour. Since periodic boundary conditions were used and k was set to be zero the energy is equivalent to the mass of the scalar particle. In fact, as stated in Section 4.2, the latter is a measure of the inverse correlation length which

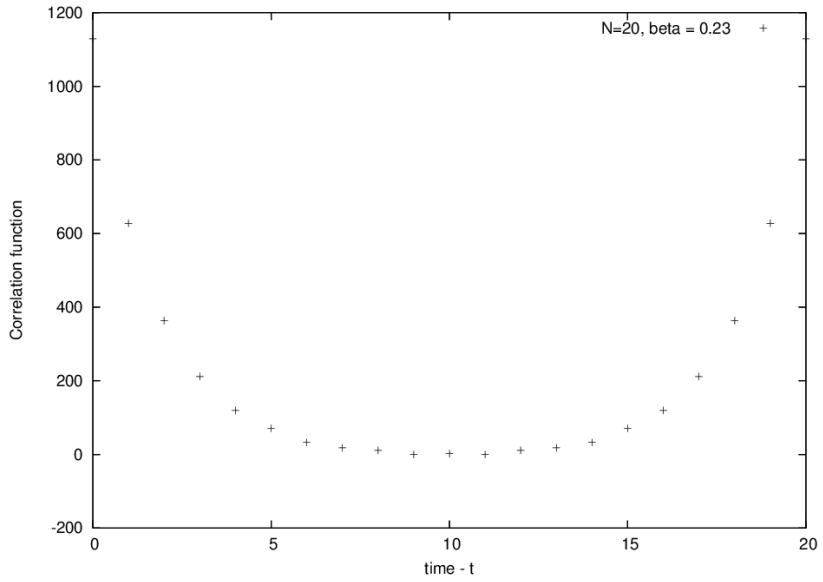

Figure 7.5: Correlation function as measured for lattice size 20 at inverse temperature $\beta = 0.23$ with periodic boundary conditions. A plateau can be seen in this case.

is given by Equation (4.25). Values of the mass were estimated by the above method and they were comparable to the values given in [30] for several inverse temperatures. This indicates that the program used to measure the correlation function is correct. A table of the masses of the scalar particle for different lattice sizes and different temperatures can be found in Appendix B.1.

For the calculations of the mass of the domain wall, the boundary conditions were set to be antiperiodic. In the calculations of the correlation function the periodicity in time direction was used to include the whole available space. Then the data of the correlation function was fitted to Equation (4.21), excluding a few points at each end to achieve the best fit. An example of how the correlation function looked like and the fitting that was achieved can be seen in Figure 7.6. Then the whole expression as given in Equation(4.26) was used, where the mass of the scalar particle as measured before was given to the program to simplify the fitting procedure. It was actually clear that the values of the mass of the domain wall, M, found using both first and second fitting, were in a good agreement.

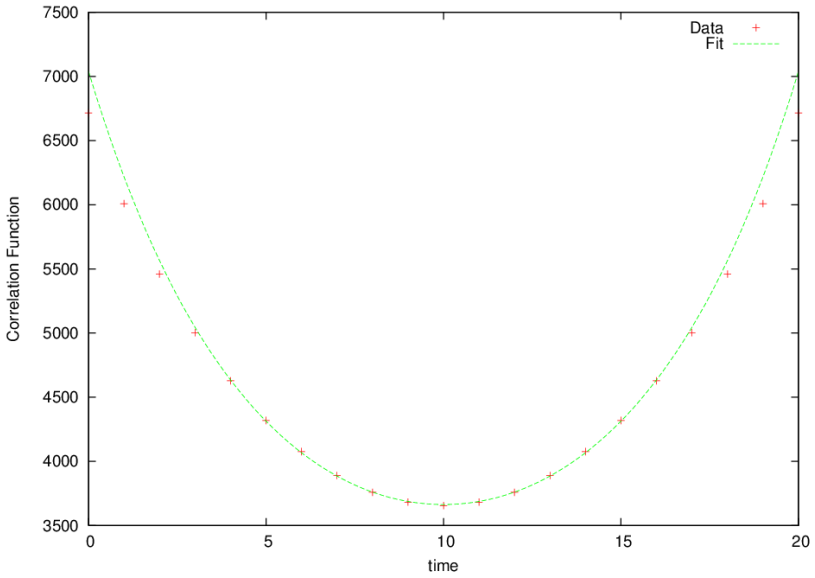

Figure 7.6: The correlation function found using the twisted boundary conditions and the fitting of the Equation (4.21) to the data points excluding 4 points from each end. The specific plot was done for lattice size $L, T = 20$ and $\beta = 0.225$

Following, the values of the mass of the domain wall found by the correlation function were compared to those found using the finite energy differences method as shown in Section 7.1. In Figure 7.7 the mass of the domain wall for two different lattice sizes as measured using both methods is shown. It is clear that there is a significant difference between the two estimated values especially at small lattice sizes. It seems that they differ by an almost constant value which might be a result of a correction term that is not taken into account.

Actually, this difference between the masses might occur due to many reasons. The most obvious one that could be investigated is the finite lattice effect. From Figure 7.7 it is noticeable that for $L = 16$ there is a bigger difference between the values compared to that of $L = 20$. This leads to the conclusion that there must be an effect from the lattice size. Even though, due to limitation in the machines and the time, the investigation of higher lattice spaces was not possible in this dissertation, the finite lattice effect was tested quantitatively using the surface tension, i.e. the mass per unit length. In principle,

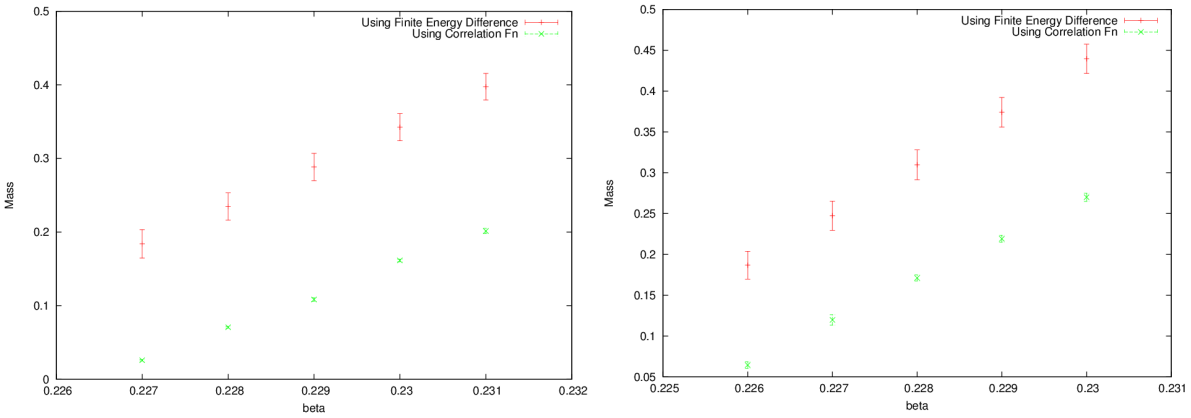

(a) N=16 **(b)** N=20

Figure 7.7: A comparison of the measured values of the mass using the two different methods for lattice sizes $N = 16$ and $N = 20$ is presented. N denotes dimensions of both time and spatial directions since a cubic lattice was considered. There is a clear difference between the values which indicates that there is a factor that has not been taken into account in the second method. This difference is smaller for higher lattice sizes so the difference might be explained by the finite lattice effect.

the surface tension should be independent of the lattice size and therefore be constant for different lattice sizes. However, due to a strong finite lattice effect, here it was observed that the surface tension was dependent on the lattice size. In the earlier calculations the surface tension was found using Equation (4.3). Also, the surface tension as measured from the mass obtained by the finite energy differences using the complete Equation (4.8) was found to be in the range of the estimated value within errors. This indicates that the first method for the mass calculations included the finite lattice effect that was imposed by the logarithmic terms. By plotting the surface tension using the masses that were obtained using both methods, it is obvious that if one goes to higher lattice sizes, they should expect to have an agreement between the values estimated using both methods. This can be seen in Figure 7.8 for two different values of the inverse temperature. This indicates that the difference that is present between the masses measured by the two different methods arises mostly from the fact that small lattices are used.

Furthermore, observing Figure 7.8, one can say that there is still a small lattice effect in the first method as well. By fitting a straight line to the values of surface tension,

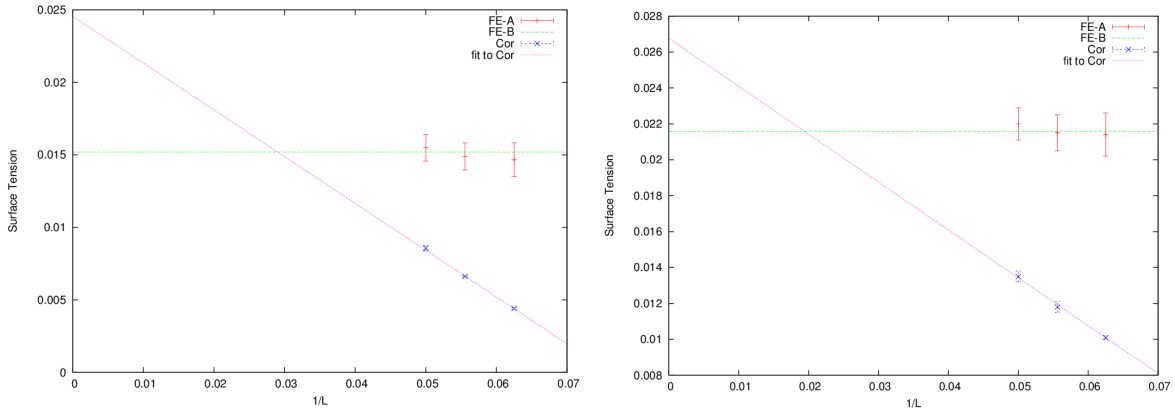

(a) $\beta = 0.228$ **(b)** $\beta = 0.23$

Figure 7.8: The surface tension as measured using the two methods across $1/L$. The straight constant line represents the surface tension that was calculated using the data of the free energy of the defect and Eq. (4.3) and the points that almost fit to this line(FE-A) represent the surface tension measured as M/L from the estimated mass by Eq. (4.8). The points given by crosses (Cor) show the surface tension, M/L, that was found using the masses obtained by the correlation function and a straight line was fitted to them. From this plot the finite lattice effect in the correlation method is apparent and it seems that if one goes to higher lattice spaces, e.g. $L = 64$ the values obtained by the two methods will agree.

M/L, using the mass found by the first method, the point where the two straight lines meet changes slightly. However, the assumption that if one goes at higher lattice sizes of $L \simeq 64$ they will get masses that should match using both methods, still holds. This is shown in Figure 7.9.

However, there might be more effects that contribute and are not taken into account in the second method resulting in giving the big difference between the masses. Even though the length of this research project does not allow further investigation, following a few of the possible explanations other than the finite lattice effect are stated. The second method was checked to be working in two models which deal with point-like particles. In the model that is presented here, the topological defect cannot be considered as point-like particle since it gets the meaning of a domain wall. Thus, there are fluctuations on the latter that are not taken into account. However, the fluctuations can be very small compared to the mass of the wall and not have a significant effect.

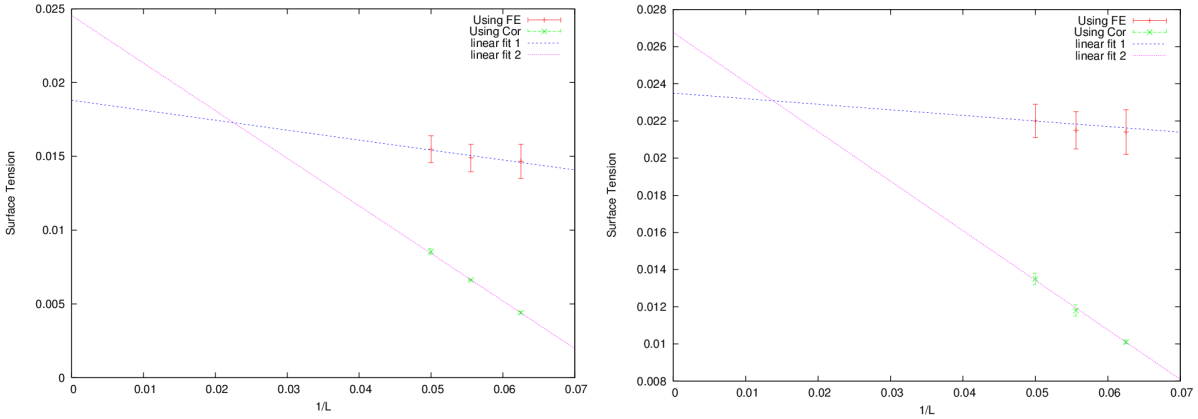

(a) $\beta = 0.228b$ **(b)** $\beta = 0.23b$

Figure 7.9: The surface tension plotted across $1/L$ using the two different methods. The investigation is similar to those in Fig. 7.8, however in this plot a straight line (linear fit 1) was fitted to the surface tension obtained using M/L where M is the mass found by the finite energy differences method. The crossing point is slightly lower in these graphs which indicates that one should go to higher lattice sizes but the assumption of $L = 64$ still holds.

Also, for the lattice sizes that were used here, the mass of the domain wall is less than the mass of the scalar particle. Therefore, there might be loop corrections in the mass of the wall that are significant and are not taken into account. Assuming that the mass grows linear with the lattice size, an extrapolation of a straight line, fitted on the masses for different lattice sizes for a specific inverse temperature, will give an idea on the size of the lattice at which the mass of the topological defect becomes almost the same as the mass of the scalar particle. The graphs for two different lattice sizes that were used for the investigation of this effect, can be found in Appendix B.2 and from those it was concluded that for the lattice size of $L = 64$ proposed above, one would most probably get values for the mass of the domain wall that are higher than the mass of the scalar particle.

Chapter 8

Conlcusion and Future Work

By the completion of this dissertation, the way of measuring the mass of topological defects with two different non-perturbative methods using Monte Carlo Simulations became clear. Specifically here, the domain wall that is created in the 1 +2-dimensional $\lambda\phi^4$ model was implemented by using the Ising Model since they live in the same universality class. In the broken phase of the Ising Model, a topological defect is created if twisted boundary conditions are imposed in one of the spatial directions.

Firstly, the mass was found by applying a widely known method which involves finite energy differences. However, for using this method one has to know the exact inverse temperature at the critical point. Thus, the first thing that was done in this dissertation was to measure this critical temperature using the Binder Cumulant for the case of periodic boundary conditions. After the critical temperature was known, the partition function of the twisted boundary conditions over the one of the periodic boundary conditions was found for small intervals of $\Delta\beta$. Then by adding the natural logarithms of these values from the critical point up to the inverse temperature that was needed, the free energy of the topological defect was obtained. Using the latter and a few logarithmic corrections, the mass of the defect was then estimated. This method works well, however, one has to deal with the problem that the computational time increases if mass measure-

ments at temperatures away from the critical one are needed. This is due to the fact that since the method is additive, with the starting point to be the critical one, the higher the temperature, the higher the number of measurements needed to be taken and added. Since, in this dissertation the mass is measured at values of the inverse temperature that are close to the critical point, good results were obtained compared to previous works.

The second method that was used involves correlation functions when the topological defect is present. For this method all the fields were transformed into momentum space and momentum took values depending on what the boundary conditions were in each direction. Specifically in x-direction $k = \pi/L$ was used whereas in time and y-direction k was set to zero. The data obtained by a program that was written to find the correlation function was fitted to the form of the latter and since momentum was known the mass could be extracted from the fit. The results obtained using this method had a similar behaviour as the results obtained using the first one, however they were not in a good agreement. Specifically there was a difference between the obtained values that appeared to be almost constant for each lattice size that was imposed.

The difference between the values of the mass obtained using the two different methods was explained by the fact that small lattice sizes were used in this dissertation. Unfortunately, the machines available for the completion of this dissertation that were used -standard computers- and the limitation of time did not allow higher lattice dimensions to be implemented and thus further investigation could not be achieved. However, in order to show that the lattice has an effect to the mass measurements, the surface tension was measured using both methods by finding the mass per unit length. In the second method it was clear that the surface tension was strongly dependent on the lattice size and by extrapolating the line that was fitted to the points, it is believed that if someone goes to higher lattice sizes, as that of $L = 64$, an agreement between the values can be achieved. Also, using small lattices, the mass of the scalar particle becomes dominant over the mass

of the defect and this might also have an effect in the mass measurement. By using the lattice size that is proposed above, as shown in Chapter 7, it is believed that it will make the mass of the domain wall higher than the mass of the scalar particle.

Even if after higher lattice sizes have been used, a disagreement between the values is still present, then one should think about other corrections that might contribute and are not taken into account. The main reason that this might happen is due to the fact that the method using the correlation functions was tested to be working in two different cases, however the defects that were present in both models that were investigated could be interpreted as point-like particles. In contradiction, in this dissertation, a domain wall is present and its string realization might add effects that are not taken into account.

The disagreement between the masses and the reasons that might causing it that are stated above unveil interesting further work that one can do. Firstly and most importantly, it is suggested that one can use a supercomputer to implement the model into larger lattices. As a first trial, my proposal is firstly, a lattice size of $L = 48$ to be used and then go into $L = 64$. Also, it will be useful to go further away from the critical point and investigate the behaviour of the mass at those temperatures. However, one has to be very careful when dealing with lower temperatures since the domain wall might gain an effect from the lattice and thus it will not be able to be interpreted as living in the continuum anymore.

Moreover, dealing with simulations is very interesting but yet very demanding on the machines and algorithms available. As it was already stated, the Metropolis Algorithm fails to give accurate results close to the critical point. Even if it is one of the simplest and well-known algorithms in the world of physics and it was sufficient for the length of this dissertation, there are more efficient algorithms that could be used to obtain better results especially close to the phase transition. In most of the papers that are mentioned

above, the Cluster Algorithm was used which gives quicker results and does not have the divergence in the error that appears close to the critical point in the Metropolis algorithm. The efficiency of these algorithms, though, has a cost in the time that they require to be written. So, as a future work for a more extended research project, a program using one of the more efficient algorithms could be written to check if there is a significant change in the results.

Overall, even though this dissertation did not give the match between the results using the two different methods, it has given the basis for further work. Either the method will work for higher lattice sizes or the method will ignore some effects that are significant and thus understanding of the underlying physics behind the topological defect in the $(\lambda\phi^4)_{1+2}$ model will open a new area of research. It is actually a really exciting topic for further investigation since, as it has already been mentioned, the specific topological defect has a relation with the confinement problem in QCD and the domain wall that it is believed that was created in the early universe. Thus, investigating it more can have applications in the theories of both cosmologists and string theorists. Hopefully, in the prospect of future work, this dissertation will have a small contribution in further investigation of the topological defects that are so important in the understanding of the behaviour of our universe.

References

[1] A. Rajantie and D. J. Weir, *Quantum kink and its excitations*, *J. High Energy Phys.*, **0904**:068, 2009

[2] L. Roters et al., *Depinning transition of a driven interface in the random- field Ising model around the upper critical dimension*, *Phys. Rev. E: Stat. Nonln. Soft Matter Phys.*, **66**:069901, 2002

[3] N. Benayad, L. Khaya and A. Fathi, *The diluted random field mixed spin Ising Model: thermodynamical properties*, *J.Phys.:Condens. Matter*, **14**:9667, 2002

[4] V. Privman *Fluctuating Interfaces, Surface Tension and Capillary Waves: An Introduction*, *Int. J. Mod. Phys.* **C3**:857, 1992

[5] G. J. Stephens, E. A. Calzetta, B. L. Hu, S.A, Ramsey *Defect Formation and Critical Dynamics in the Early Universe*, *Phys. Rev. D*, **59**:045009, 1999

[6] B. M. McCoy and T. Tsun Wu *The two-dimensional Ising Model*, Harvard University Press, Cambridge, Massachussets, 1973

[7] F. Canfora *Kallen-Lehman approach to 3D Ising Model*, *Phys. Lett. B*, **646**:54, 2007

[8] M. Caselle, M. Hasenbusch, P. Provero and K. Zarembo, *Bound states in the three-dimensional ϕ^4 model*, *Phys. Rev. D*, **62**:017901, 2000

[9] M. Caselle, M. Hasenbusch, P. Provero and K. Zarembo *Bound states and glueballs in three-dimensional Ising systems*, *Nucl. B*, **623**:474, 2002

[10] L. P. Kadanoff, *Operator Algebra and the determination of critical indices*, *Phys. rev. Lett.*, **23**:1430, 1969

[11] L. P. Kadanoff and H. Ceva *Determination of an Operator Algebra for the two dimensional Ising Model*, *Phys. Rev. B*, **3**:3918, 1971

[12] J. C. Ciria, A. Tarancon, *Renormalization Group Study of the soliton mass on the* $(\lambda\Phi^4)_{1+1}$ *lattice model*, *Phys. Rev. D*, **49**:1020, 1994

[13] A. C. Davis, T. W. B. Kibble, A. Rajantie and H. P. Shanahan, *Topological defects in lattice gauge theories*, *J. High Energy Phys.*, **11**:010, 2000

[14] G. t' Hooft, *On the phase transition towards permanent quark confinement*, *Nucl. Phys. B*, **138**:1, 1978

[15] G. t' Hooft, *A property of electric and magnetic flux in non-abelian gauge theories*, *Nucl. Phys. B* **153**:141, 1979

[16] B. Svetitsky and L. G. Yaffe, *Critical behavior at finite-temperature confinement transitions Nucl. Phys. B*, **210**:423, 1982

[17] M. Pepe and Ph. De Forcrand *Finite-size scaling of interface free energies in the 3D Ising model*, *Nucl.Phys.Proc.Suppl.*, **106**:914, 2002

[18] A. M. Polyakov, *Thermal properties of gauge fieldsand quark liberation*, *Phys. Lett. B*, **72**:477, 1978

[19] L. Susskind, *Lattice models of quark confinement at high temperature*, *Phys. Rev. D*, **20**:2610, 1979

[20] Ph. De Forcrand and L. Von Smekal, *'t Hooft loops and consistent order parameters for confinement*, *Nucl.Phys.Proc.Suppl.*, **106**:619, 2002

[21] Ph. De Forcrand and L. Von Smekal, *'t Hooft loops, electric flux sectors and Confinement in* $SU(2)$ *Yang-Mills Theory*, *Phys. Rev. D*, **66**:011504, 2002

[22] K. Holland and U-J. Wiese, *The center symmetry and its spontaneous breakdown at high temperatures*, 2000 [hep-ph/0011193v1]

[23] D. A. Kirzhnits, *Weinberg Model and the 'Hot' Universe JETP Letters*, **15**:745, 1972

[24] D. A. Kirzhnits and A. D. Linde, *Macroscopic consequences of the Weinberg model Phys. Lett.*, **42**:471 , 1974

[25] L. Dolan, and R. Jackiw, *Symmetry behavior at finite temperature*, *Phys. Rev. D*, **9**:3320, 1974

[26] S. Weinberg, *Gauge and global symmetries at high temperatures*, *Phys. Rev. D*, **9**:3357, 1974

[27] T. W. B. Kibble, *Topology of cosmic domains and strings*, *J. Phys. A: Math. Gen.*, **9**:1387, 1976

[28] J. Groeneveld, J. Jurkiewicz and C. P. Korthals Altes, *Twist as a Probe for Phase Structure*, *Physica Scripta*, **23**:1022, 1981

[29] M. Hasenbusch *Direct Monte Carlo measurement of the surface tension in Ising Models*, [arXiv:hep-lat/9209016], 1992

[30] M. Hasenbusch, K. Pinn, *Surface tension, surface stiffness, and surface width of the 3-dimensional Ising Model on a cubic lattice*, *Physica A.*, **192**:342, 1993

[31] M. Caselle, M. Hasenbusch and M. Panero, *High precision Monte Carlo simulations of interfaces in the three-dimensional Ising model: a comparison with the Nambu-Goto effective string model*, *J. High Energy Phys.*, **063**:084, 2006

[32] M. Hasenbusch and K. Pinn *Comparison of Monte Carlo Results for the 3D Ising Interface Tension and Interface Energy with (Extrapolated) Series Expansions*, *Physica A*, **203**:189, 1994

[33] J. D. Weeks, G. H. Gilmer, M. J. Leamy *Structural Transition in the Ising-Model Interface*, *Phys. Rev. Lett.*, **31**:549, 1973

[34] H. Arisue, preprint OPCT 93-1, May 1993

[35] A. Rajantie and D. Weir *Nonperturbative study of the t Hooft-Polyakov monopole form factors*,[arXiv:hep-lat/1109.0299v1], 2011

[36] A. Rajantie and D. J. Weir *Soliton form factors from lattice simulations*, *Phys. Rev. D*, **82**:111502, 2010

[37] N. Metropolis, A. W. Rosenbluth, M. N. Rosenbluth, A. H. Teller, and E. Teller., *Equation of Sate Calculations by Fast Computing Machines*, *J. Chem. Phys.*, **21**:1087, 1953

[38] M. E. J. Newman and G. T. Barkema, *Monte Carlo Methods in Statistical Physics*, Oxford University Press Inc., New York, USA, 1999

[39] A. K. Hartmann and H. Rieger, *New Optimization Algorithms in Physics*, Wiley-VCH, Berlin, 2004

[40] N. Goldenfeld, *Lectures on Phase Transitions and The Renormalization Group*, Westview Press, University of Illionois, 1992

[41] K. Binder *Critical properties from Monte Carlo coarse graining and renormalisation*, *Phys. Rev. Lett.*, **47**:693, 1981

[42] J. Adler *Critical Temperature of the d=3 s=1/2 Ising Model: the effect of confluent corrections to scaling*, *J. Phys. A*, **16**:3585, 1983

[43] A. L. Talapov and H. W. J. Blote *The magnetization of the 3D Ising Model*, J. Phys. A, **29**:5727, 1996

[44] F. Livet, *The Cluster Updating Monte Carlo Algorithm applied to the 3D Ising problem*, *Europhys. Lett.*, **16**:139, 1991

[45] A. Rajantie, *Mass of a quantum 't Hooft-Polyakov monopole*, *J. High Energy Phys.*, **01**:088, 2006

[46] M. Caselle, M. Hasenbusch and M. Panero, *The interface free energy: Comparison of accurate Monte Carlo results for the 3D Ising model with effective interface models*, *J. High Energy Phys.*, **09**:117, 2007

Appendix A

Finding the mass of a topological defect using the free energy

In this appendix, the explicit derivation of Equation (4.8) given in Section 4.1 is shown. Equations (4.5), (4.6) and (4.7) were used.

$$\begin{aligned}
\Delta F &= -\ln \frac{Z_{TW}}{Z_P} \\
&= -\ln \left(\frac{2Z_0 \left(Z_1 e^{-MT} + \frac{1}{3!} Z_1^3 e^{-3MT} + .. \right)}{Z_0 \left(1 + Z_1^2 e^{-2MT} + ... \right)} \right) \\
&= \ln 2 - \ln \left(\frac{Z_1 e^{-MT} + \frac{1}{3!} Z_1^3 e^{-3MT}}{1 + Z_1^2 e^{-2MT}} \right) \\
&= -\ln 2 - \ln \left(\frac{Z_1 e^{-MT}}{1 + Z_1^2 e^{-2MT}} \right) + O(e^{-2MT}) \\
&= -\ln 2 - \ln \left(Z_1 e^{-MT} \right) + \ln(1 + Z_1^2 e^{-2MT}) + O(e^{-2MT}) \\
&= -\ln 2 - \ln Z_1 + MT + O(e^{-2MT}) \\
&= MT - \ln 2 - \frac{1}{2} \ln \left(\frac{ML^2}{2\pi T} \right) + O(e^{-2MT})
\end{aligned}$$

where in the final result was obtained by substituting the definition of Z_1 as :

$$Z_1 = \left(\frac{ML^2}{2\pi T} \right)^{1/2}.$$

Appendix B

Further Results

B.1 Mass of scalar particle

β \ N	14	16	18	20
0.225	0.281 ±0.003	0.285 ±0.005	0.285 ±0.003	0.285 ±0.008
0.226	0.329 ±0.017	0.321 ±0.005	0.328 ±0.003	0.329 ±0.005
0.227	0.388 ±0.007	0.392 ±0.004	0.400 ±0.004	0.396 ±0.005
0.228	0.426 ±0.004	0.425 ±0.003	0.417 ±0.007	0.429 ±0.009
0.229	0.477 ±0.006	0.476 ±0.016	0.479 ±0.005	0.475 ±0.007
0.230	0.507 ±0.005	0.507 ±0.018	0.508 ±0.004	0.509 ±0.009

Table B.1: The mass of the scalar particle as measured using the correlation function with periodic boundary conditions. It can be seen that varying the lattice size but keeping the temperature constant the value of the mass of the scalar particle remains the same within errors.

B.2 Investigation of relation between mass of topological defect and mass of scalar particle

The two graphs that are presented here are those discussed in Section 7.2. It is clear that by extrapolating the straight line that fits the values for the masses obtained, there is a point at which it crosses the line which represents the mass of the scalar particle. This crossing point roughly indicates the critical lattice size that one should use to achieve a mass of the defect higher than that of the scalar particle. If the mass of the domain wall is much larger than the scalar particle, then any corrections that are not taken into account will be very small and thus not contribute in the estimation of the mass of the defect. Although, it is clear that this lattice size depends on the temperature, one can take a safe limit of $L = 50$ to be considered as a lattice size that would result in a dominant mass of the topological defect over the mass of the boson.

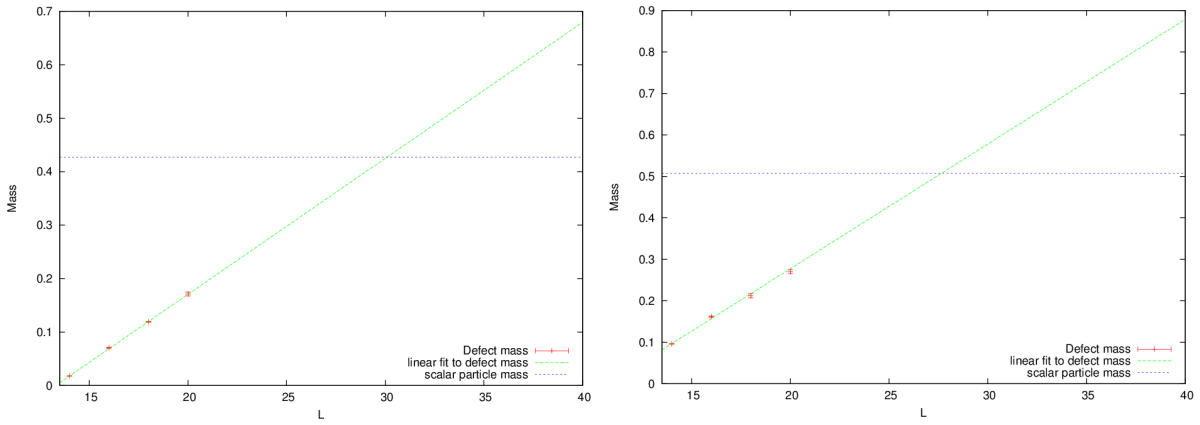

(a) $\beta = 0.228$ **(b)** $\beta = 0.23$

Figure B.1: The mass of the domain wall and a linear fit to the data points across the lattice size is shown here. The line which is constant for all values of L indicates the mass of the scalar particle. At higher lattice size the mass of the domain wall becomes dominant.

Appendix C

Programs used in this dissertation

C.1 Program for implementing the Ising Model

The main program presented here is an original work of the author and it was written in FORTRAN 95. However, the function to generate random numbers was taken from a report that was found online. Periodic Boundary conditions were used in the specific program.

```
PROGRAM ising_3D
implicit none
!-------------------------------------------------------------------------
!3D ISING MODEL using Metropolis Algorithm - periodic boundary conditions
!-------------------------------------------------------------------------
!
!-------------------------------------------------------------------------
!Variables
!-------------------------------------------------------------------------
integer :: i,j,k,m,n,p
real:: Je = 1.0
integer, allocatable :: A(:,:,:), ER(:)
real, allocatable :: E(:,:,:)
integer :: n1,n2,n3, ConfigType
real :: temp, beta, high_temp, low_temp, temp_interval
integer :: npass, ipass, nequil, trial_spin, steps
integer :: nscans, iscan, output_count
real :: log_eta, deltaU, tauto
real :: magn, magn_ave, magn2_ave, magn4_ave, dm, dm2, varianceM, varianceM2
real :: E_ave, E2_ave, E4_ave, energy, dE, dE2, varianceE, varianceE2
real :: cv, dcv, dchi, chi

!-------------------------------------------------------------------------
!Reading initial parameters, defined by the user, from a file
!input file = 'ising.txt'
!-------------------------------------------------------------------------
open (unit = 11, file = 'ising.txt',status = 'old', action = 'read')

read(11,*); read(11,*) n1
read(11,*); read(11,*) n2
read(11,*); read(11,*) n3
read(11,*); read(11,*) npass
```

```
read(11,*); read(11,*) nequil
read(11,*); read(11,*) high_temp
read(11,*); read(11,*) low_temp
read(11,*); read(11,*) temp_interval
read(11,*); read(11,*) ConfigType

close (11)

steps = 1500

nscans = int((high_temp - low_temp)/temp_interval) + 1

!-------------------------------------------------------------------------
!Allocate array of spins, energy and errors
!-------------------------------------------------------------------------

allocate (A(n1+2, n2+2, n3+2))
allocate (E(n1+2, n2+2, n3+2))
allocate (ER(nscans))

!-------------------------------------------------------------------------
!Output files: energy.dat, magnetization.dat
!-------------------------------------------------------------------------

open (unit = 33, file = 'magnetization.dat', status = 'replace', action = 'write')

open (unit=34, file = 'energy.dat', status = 'replace', action = 'write')

!-------------------------------------------------------------------------
!Read the autocorrelation function for each temp from a file
!-------------------------------------------------------------------------
open (unit=37, file = 'error20.txt',status = 'old', action = 'read')

do i=1, nscans
 read(37,*) ER(i)
end do

close (37)

!-------------------------------------------------------------------------
!Initial spin configuration - depends on ConfigType given
!-------------------------------------------------------------------------
 select case (ConfigType)

  case(1) !completely ordered + 1

   do i=1, n1+2
     do j=1, n2+2
       do k=1, n3+2
         A(i,j,k) = 1
       end do
     end do
   end do
```

```
  case(2) !random configuration
    do i=2, n1+1
      do j=2, n2+1
        do k=2, n3+1
          if (ran1(5)>0.5) then
            A(i,j,k)=1
            write(32,*) A(i,j,k)
          else
            A(i,j,k)=-1
            Write(32,*) A(i,j,k)
         end if
        end do
       end do
     end do
     A(1,:,:) = 1
     A(n1+2,:,:) = 1
     A(:,1,:) = 1
     A(:,n2+2,:) = 1
     A(:,:,1) = 1
     A(:,:,n3+2) = 1

  case(3) !checkerboard

    do i=2, n1+1
      do j=2, n2+1
        do k=2, n3+1
          if (mod(i+j+k,2).eq.0) then
            A(i,j,k) = 1
          else
            A(i,j,k) = -1
          end if
        end do
      end do
    end do
    A(1,:,:) = 1
    A(n1+2,:,:) = -1
    A(:,1,:) = 1
    A(:,n2+2,:) = -1
    A(:,:,1) = 1
    A(:,:,n3+2) = -1

  case default
  print*, 'Error! Check ConfigType'
  stop
  end select

!-----------------------------------------------------------------------
!Loop for each temp interval (from high to low)
!-----------------------------------------------------------------------

 scan_loop: do iscan = 1, nscans
   write(*,*) iscan
   temp = high_temp - temp_interval *(iscan-1)
   beta = 1.0/temp
!-----------------------------------------------------------------------
```

```
!Metropolis algorithm
!-------------------------------------------------------------------------------
   magn_ave = 0.0
   magn2_ave = 0.0
   magn4_ave = 0.0
   E_AVE = 0.0
   E2_AVE =0.0
   E4_AVE = 0.0
   output_count =0

   MC_passes : do ipass =1, npass

!Choose a random spin i->m, j->n, k->p and flip sign

     m = nint((n1-1)*ran1(5) + 2)
     n = nint((n2-1)*ran1(5) + 2)
     p = nint((n3-1)*ran1(5) + 2)
     trial_spin = -A(m,n,p)

!Energy change after flipping
     deltaU = -Je*float(2*trial_spin*(A(m-1,n,p)+A(m+1,n,p)+A(m,n-1,p)+A(m,n+1,p)
       +A(m,n,p-1)+A(m,n,p+1)))

     if (deltaU.le.0) then
       A(m,n,p) = trial_spin
     else
       log_eta = log(ran1(5))
       if (-beta*deltaU.gt.log_eta) then
         A(m,n,p) = trial_spin
       end if
     end if

!Fix the boundaries to be periodic

     if ((deltaU.le.0).or.((deltaU.gt.0).and.(-beta*deltaU.gt.log_eta))) then
       if (m==2) A(n1+2,n,p)= trial_spin
       if (m==n1+1) A(1,n,p) = trial_spin
       if (n==2) A(m, n2+2,p) = trial_spin
       if (n==n2+1) A(m,1,p) = trial_spin
       if (p==2) A(m,n,n3+2) = trial_spin
       if (p==n3+1) A(m,n,1) = trial_spin
     end if

!-------------------------------------------------------------------------------
!All calculations that we want after equilibration and every '1500' steps
!-------------------------------------------------------------------------------

     if ((ipass.gt.nequil).and.(mod(ipass,steps).eq.0)) then
       output_count = output_count + 1

!Magnetization calculations
       magn = sum(A(2:n1+1,2:n2+1,2:n3+1))
       magn_ave = magn_ave + magn/(n1*n2*n3)
       magn2_ave = magn2_ave + (magn/(n1*n2*n3))**2
       magn4_ave = magn4_ave + (magn/(n1*n2*n3))**4
```

```
!Energy calculations
      energy = 0.0
      do i=2, n1+1
        do j=2, n2+1
          do k=2, n3+1
           E(i,j,k)=-Je*float(A(i,j,k)*(A(i-1,j,k)+A(i+1,j,k)+A(i,j-1,k)
                    +A(i,j+1,k)+A(i,j,k-1)+A(i,j,k+1)))
           energy = energy + E(i,j,k)/2
          end do
        end do
      end do
      E_AVE = E_AVE + energy/(n1*n2*n3)
      E2_AVE = E2_AVE + (energy/(n1*n2*n3))**2
      E4_AVE = E4_AVE + (energy/(n1*n2*n3))**4

     end if

   end do MC_passes

   magn_ave = magn_ave/(output_count*n1*n2*n3)
   magn2_ave = magn2_ave/(output_count)
   magn4_ave = magn4_ave/(output_count)
   chi = beta*(magn2_ave - (magn_ave)**2)

   E_AVE = E_AVE/(output_count*n1*n2*n3)
   E2_AVE = E2_AVE /(output_count)
   E4_AVE = E4_AVE /(output_count)
   cv = beta**2*(E2_AVE -(E_AVE**2))

   tauto = ER(iscan)

   varianceM = magn2_ave - magn_ave**2
   varianceM2 = magn4_ave - magn2_ave**2

   dm = sqrt((varianceM*(2*tauto))/(output_count))
   dm2 = sqrt((varianceM2*(2*tauto))/(output_count))

   varianceE = E2_ave - E_ave**2
   varianceE2 = E4_ave - E2_ave**2
   dE = sqrt((varianceE*(2*tauto))/(output_count))
   dE2 = sqrt((varianceE2*(2*tauto))/(output_count))

   dchi = beta*sqrt(dm2**2+4*(magn_ave*dm)**2)
   dcv = beta**2*sqrt(dE2**2+4*(E_ave*dE)**2)


   write(33,*) temp, ABS(magn_ave), dm, chi , dchi

   write(34,*) temp, E_AVE, dE, cv, dcv

 end do scan_loop

 close(33)
 close(34)
```

```
 print*, 'Program complete'
 print*, 'Check energy.dat and magnetization.dat'


!-----------------------------------------------------------------------
! Function to generate random number
!-----------------------------------------------------------------------
contains

real function ran1(idum)
implicit none

real :: r(97)
integer, intent(IN) :: idum
save
integer, parameter :: M1=259200, IA1=7141, IC1=54773
real, parameter :: RM1=1.0d0/M1
integer, parameter :: M2=134456, IA2=8121, IC2=28411
real, parameter :: RM2=1.0d0/M2
integer, parameter :: M3=243000, IA3=4561, IC3=51349
integer :: IX1, IX2, IX3, jjj
integer :: iff=0

if (idum<0.or.iff==0) then
  iff = 1
  IX1 = mod(IC1-idum, M1)
  IX1 = mod(IA1*IX1+IC1, M1)
  IX2 = mod(IX1, M2)
  IX1 = mod(IA1*IX1+IC1,M1)
  IX3 = mod(IX1, M3)

  DO jjj =1,97
    IX1 = mod(IA1*IX1+IC1, M1)
    IX2 = mod(IA2*IX2+IC2, M2)
    r(jjj) = (float(IX1) + float(IX2)*RM2)*RM1
  END DO

END IF

IX1 = mod(IA1*IX1+IC1, M1)
IX2 = mod(IA2*IX2+IC2, M2)
IX3 = mod(IA3*IX3+IC3, M3)
jjj = 1+(97*IX3)/M3
if (jjj >97.or.jjj <1) PAUSE
ran1 = r(jjj)
r(jjj) = (float(IX1)+float(IX2)*RM2)*RM1

end function ran1

end program ising_3D
```

C.2 Program for finding the mass using correlation functions

Manipulating the program given in Appendix C.1, the correlation function of the fields, in the case of this dissertation the spins, was found. By fitting the data extracted from this program to Equation 4.26, the mass of the domain wall could be calculated.

```
PROGRAM correlation
implicit none
!-------------------------------------------------------------------------------
!Program to find the correlation function in order to find the mass.
!It uses the Ising Model, Monte Carlo Simulations with Metropolis Algorithm
!and twisted boundary conditions in x-direction.
!-------------------------------------------------------------------------------
!
!-------------------------------------------------------------------------------
!Variables
!-------------------------------------------------------------------------------
integer :: i,j,k,m,n,p
integer, parameter :: ik = selected_int_kind (16)
real :: pi = 3.14159265
real:: Je = 1.0
integer, allocatable :: A(:,:,:)
real, allocatable :: E(:,:,:), FT(:,:), C(:,:), iS(:) , S(:), eC(:,:)
integer :: n1,n2,n3, ConfigType
real :: temp, beta, kmom, tauto
integer :: trial_spin, steps
integer (kind=ik) :: npass, ipass, nequil
real :: high_temp, low_temp, temp_interval
integer :: nscans, iscan, output_count
real :: log_eta, deltaU
real :: cor, icor, cor2, icor2, dcor, dcor2, idcor, idcor2
real :: sumS, sumS2, dsumS

!-------------------------------------------------------------------------------
!Reading initial parameters, defined by the user, from a file
!input file = 'info.txt'
!-------------------------------------------------------------------------------
open (unit = 11, file = 'info.txt',status = 'old', action = 'read')

read(11,*); read(11,*) n1
read(11,*); read(11,*) n2
read(11,*); read(11,*) n3
read(11,*); read(11,*) npass
read(11,*); read(11,*) nequil
read(11,*); read(11,*) beta
read(11,*); read(11,*) tauto
read(11,*); read(11,*) ConfigType

close (11)

temp = 1/beta
steps = 10000
```

```
WRITE(*,*) 'N = ', n1
WRITE(*,*) 'temp = ',temp

!-------------------------------------------------------------------------------
!Allocate arrays
!-------------------------------------------------------------------------------

allocate (A(n1+2, n2+2, n3+2))
allocate (S(n3+2))
allocate (iS(n3+2))
allocate (FT(n1+2,2))
allocate (C(n3+2,2))
allocate (eC(n3+2,2))


!-------------------------------------------------------------------------------
!Create array with the fourier transform values - k = constant
!-------------------------------------------------------------------------------

kmom = pi/n3

do i =1, n1
  FT(i,1) = cos(kmom*(i-1))
  FT(i,2) = sin(kmom*(i-1))
  WRITE(*,*) FT(i,1)
end do
FT(n1+1, 1) = FT(1,1)
FT(n1+1, 2) = FT(1,2)
FT(n1+2, 1) = FT(2,1)
FT(n1+2, 2) = FT(2,2)


!-------------------------------------------------------------------------------
!Output file: cor.dat and icor.dat
!-------------------------------------------------------------------------------

open (unit = 38, file = 'cor.dat')

open (unit = 39, file  ='icor.dat')

!-------------------------------------------------------------------------------
!Initial spin configuration - depends on ConfigType given
!-------------------------------------------------------------------------------
 select case (ConfigType)

  case(1) !completely ordered + 1

   do i=1, n1+2
     do j=1, n2+2
       do k=1, n3+2
         A(i,j,k) = 1
       end do
     end do
   end do
```

```
  case(2) !random configuration
    do i=2, n1+1
      do j=2, n2+1
        do k=2, n3+1
          if (ran1(5)>0.5) then
            A(i,j,k)=1
            write(32,*) A(i,j,k)
          else
            A(i,j,k)=-1
            Write(32,*) A(i,j,k)
          end if
        end do
      end do
    end do
    A(1,:,:) = 1
    A(2,:,:) = 1
    A(n1+1,:,:) = -1
    A(n1+2,:,:) = -1
    A(:,1,:) = 1
    A(:,2,:) = 1
    A(:,n2+2,:) = 1
    A(:,n2+1,:) = 1
    A(:,:,1) = 1
    A(:,:,2) = 1
    A(:,:,n3+1) = 1
    A(:,:,n3+2) = 1

  case(3) !checkerboard

    do i=2, n1+1
      do j=2, n2+1
        do k=2, n3+1
          if (mod(i+j+k,2).eq.0) then
            A(i,j,k) = 1
          else
            A(i,j,k) = -1
          end if
        end do
      end do
    end do
    A(1,:,:) = 1
    A(n1+2,:,:) = -1
    A(:,1,:) = 1
    A(:,n2+2,:) = -1
    A(:,:,1) = 1
    A(:,:,n3+2) = -1

  case default
  print*, 'Error! Check ConfigType'
  stop
  end select

!-----------------------------------------------------------------------
!Metropolis algorithm
```

```
!-----------------------------------------------------------------------

output_count =0
C(:,:) = 0
eC(:,:) = 0

MC_passes : do ipass =1, npass

!Choose a random i->m, j->n, k->p and flip sign
  m = nint((n1-1)*ran1(5) + 2)
  n = nint((n2-1)*ran1(5) + 2)
  p = nint((n3-1)*ran1(5) + 2)
  trial_spin = -A(m,n,p)

!Energy change after flipping
  deltaU = -Je*float(2*trial_spin*(A(m-1,n,p)+A(m+1,n,p)+A(m,n-1,p)+A(m,n+1,p)+A(m,n,p-1

  if (deltaU.le.0) then
    A(m,n,p) = trial_spin
  else
    log_eta = log(ran1(5))
    if (-beta*deltaU.gt.log_eta) then
      A(m,n,p) = trial_spin
    end if
  end if

!Fix the boundaries to be anti periodic in x-direction
  if ( (deltaU.le.0).or.((deltaU.gt.0).and.(-beta*deltaU.gt.log_eta)) ) then
    if (m==2) A(n1+2,n,p)= -trial_spin
    if (m==n1+1) A(1,n,p) = -trial_spin
    if (n==2) A(m, n2+2,p) = trial_spin
    if (n==n2+1) A(m,1,p) = trial_spin
    if (p==2) A(m,n,n3+2) = trial_spin
    if (p==n3+1) A(m,n,1) = trial_spin
  end if

!-----------------------------------------------------------------------
!All calculations that we want after equilibration and every '1500' steps
!-----------------------------------------------------------------------

  if ((ipass>nequil).and.(mod(ipass,steps)==0)) then
    output_count = output_count + 1

!-----------------------------------------------------------------------
!Do fourier transform of the spins - for every t i.e k
!-----------------------------------------------------------------------
    S(:) = 0
    iS(:) = 0
    sumS = 0.0
    sumS2 = 0.0
      do k=1, n3
        do i=1, n1
          do j=1, n2
            S(k) = S(k) + FT(i,1)*A(i,j,k)
            iS(k) = iS(k) + FT(i,2)*A(i,j,k)
```

```
            end do
          end do
          sumS = sumS + S(k)
          sumS2 = sumS2 + S(k)**2
        end do

      sumS = sumS/n3
      sumS2 = sumS2/n3
      dsumS = sqrt((sumS2 - sumS**2)/(n3*(n3+1)))

!-------------------------------------------------------------------------
!Find the correlation function using periodicity in time direction - k
!-------------------------------------------------------------------------
      do m=0, n3

        cor =0.0
        icor = 0.0
        cor2 =0.0
        icor2 = 0.0

        do k=0, n3-1
         cor = cor + S(k+1)*S(mod(k+m,n3)+1)+iS(k+1)*iS(mod(k+m,n3)+1)
         cor2 = cor2 + (S(k+1)*S(mod(k+m,n3)+1)+iS(k+1)*iS(mod(k+m,n3)+1))**2
         icor = icor + iS(k+1)*S(mod(k+m,n3)+1) - S(k+1)*iS(mod(k+m,n3)+1)
         icor2 = icor2 + (iS(k+1)*S(mod(k+m,n3)+1) - S(k+1)*iS(mod(k+m,n3)+1))**2
        end do

        cor2 = cor2/n3
        cor = cor/n3
        dcor = sqrt((cor2 - cor**2)/(n3*(n3-1)))
        cor = cor- sumS**2

        icor2 = icor2/n3
        icor = icor/n3
        idcor = sqrt((icor2 - icor**2)/(n3*(n3-1)))

        dcor2 = dcor**2+ (2*sumS*dsumS)**2
        idcor2 = idcor**2+ (2*sumS*dsumS)**2

       C(m+1,1) = C(m+1,1)+ cor
       eC(m+1,1) = eC(m+1,1) + dcor2
       C(m+1,2) = C(m+1,2) + icor
       eC(m+1,2) = eC(m+1,2) + idcor2

      end do

    end if

end do MC_passes

do m=0, n3
    C(m+1,1) = C(m+1,1)/output_count
    C(m+1,2) = C(m+1,2)/output_count
    eC(m+1,1) = sqrt((eC(m+1,1)*tauto)/output_count)
    eC(m+1,2) = sqrt((eC(m+1,2)*tauto)/output_count)
```

```
  WRITE(38,*) m, C(m+1,1), eC(m+1,1)
  WRITE(39,*) m, C(m+1,2), eC(m+1,2)
end do

close(38)
close(39)

deallocate(A)
deallocate(FT)
deallocate(S)
deallocate(iS)
deallocate(C)
deallocate(eC)

print*, 'Program complete'
print*, 'Data saved in cor.dat and icor.dat'


!-----------------------------------------------------------------------
! Function to generate random number
!-----------------------------------------------------------------------
contains

real function ran1(idum)
implicit none

real :: r(97)
integer, intent(IN) :: idum
save
integer, parameter :: M1=259200, IA1=7141, IC1=54773
real, parameter :: RM1=1.0d0/M1
integer, parameter :: M2=134456, IA2=8121, IC2=28411
real, parameter :: RM2=1.0d0/M2
integer, parameter :: M3=243000, IA3=4561, IC3=51349
integer :: IX1, IX2, IX3, jjj
integer :: iff=0

if (idum<0.or.iff==0) then
  iff = 1
  IX1 = mod(IC1-idum, M1)
  IX1 = mod(IA1*IX1+IC1, M1)
  IX2 = mod(IX1, M2)
  IX1 = mod(IA1*IX1+IC1,M1)
  IX3 = mod(IX1, M3)

  DO jjj =1,97
    IX1 = mod(IA1*IX1+IC1, M1)
    IX2 = mod(IA2*IX2+IC2, M2)
    r(jjj) = (float(IX1) + float(IX2)*RM2)*RM1
  END DO

END IF

IX1 = mod(IA1*IX1+IC1, M1)
IX2 = mod(IA2*IX2+IC2, M2)
```

```
IX3 = mod(IA3*IX3+IC3, M3)
jjj = 1+(97*IX3)/M3
if (jjj>97.or.jjj<1) PAUSE
ran1 = r(jjj)
r(jjj) = (float(IX1)+float(IX2)*RM2)*RM1

end function ran1

end program correlation
```